PCT

WORLD INTELLECTUAL PROPERTY ORGANIZATION
International Bureau

INTERNATIONAL APPLICATION PUBLISHED UNDER THE PATENT COOPERATION TREATY (PCT)

(51) International Patent Classification 6 : G01N 23/04	A1	(11) International Publication Number: WO 99/42818 (43) International Publication Date: 26 August 1999 (26.08.99)

(21) International Application Number: PCT/US99/03269

(22) International Filing Date: 17 February 1999 (17.02.99)

(30) Priority Data:
09/027,605 23 February 1998 (23.02.98) US

(71) Applicant: NICOLET IMAGING SYSTEMS [US/US]; Suite F, 8221 Arjons Drive, San Diego, CA 92126 (US).

(72) Inventors: THAYER, Dale, D.; 17755 Pennacook Court, San Diego, CA 92127 (US). DUFF, Eric, A.; 1242 River Glen Row #42, San Diego, CA 92111 (US). BOWLES, Philip, H.; 120 Maplecrest Drive, Carmel, IN 46033 (US). SMITH, Steven, W.; 16129 Bennye Lee Drive, Poway, CA 92064 (US). AXFORD, Paul, J.; 10905 Canyon Mesa Lane, San Diego, CA 92126 (US). YARNALL, Ransom, A.; 9257 Virginia Lane, La Mesa, CA 91941 (US).

(74) Agent: SAMPSON, Matthew, J.; McDonnell, Boehnen, Hulbert & Berghoff, Suite 3200, 300 South Wacker Drive, Chicago, IL 60606 (US).

(81) Designated States: AL, AM, AT, AU, AZ, BA, BB, BG, BR, BY, CA, CH, CN, CU, CZ, DE, DK, EE, ES, FI, GB, GD, GE, GH, GM, HR, HU, ID, IL, IN, IS, JP, KE, KG, KP, KR, KZ, LC, LK, LR, LS, LT, LU, LV, MD, MG, MK, MN, MW, MX, NO, NZ, PL, PT, RO, RU, SD, SE, SG, SI, SK, SL, TJ, TM, TR, TT, UA, UG, UZ, VN, YU, ZW, ARIPO patent (GH, GM, KE, LS, MW, SD, SZ, UG, ZW), Eurasian patent (AM, AZ, BY, KG, KZ, MD, RU, TJ, TM), European patent (AT, BE, CH, CY, DE, DK, ES, FI, FR, GB, GR, IE, IT, LU, MC, NL, PT, SE), OAPI patent (BF, BJ, CF, CG, CI, CM, GA, GN, GW, ML, MR, NE, SN, TD, TG).

Published

With international search report.
Before the expiration of the time limit for amending the claims and to be republished in the event of the receipt of amendments.

(54) Title: METHOD AND APPARATUS FOR IMAGING OBSCURED AREAS OF A TEST OBJECT

(57) Abstract

A method and apparatus for imaging a region of interest that is positioned on or within a test object (14). The method includes the step of generating a radiation beam (24), such as an x-ray beam. The method further includes the step of directing the radiation beam to a discrete number of predetermined locations on the test object. The predetermined locations are preferably selected to produce an unobscured electronic image of the region of interest. The discrete number of predetermined locations is minimized while being of sufficient number to produce the unobscured electronic image. The apparatus includes a radiation source (2) and a device for directing the radiation from the source to a discrete number of predetermined locations on a test object.

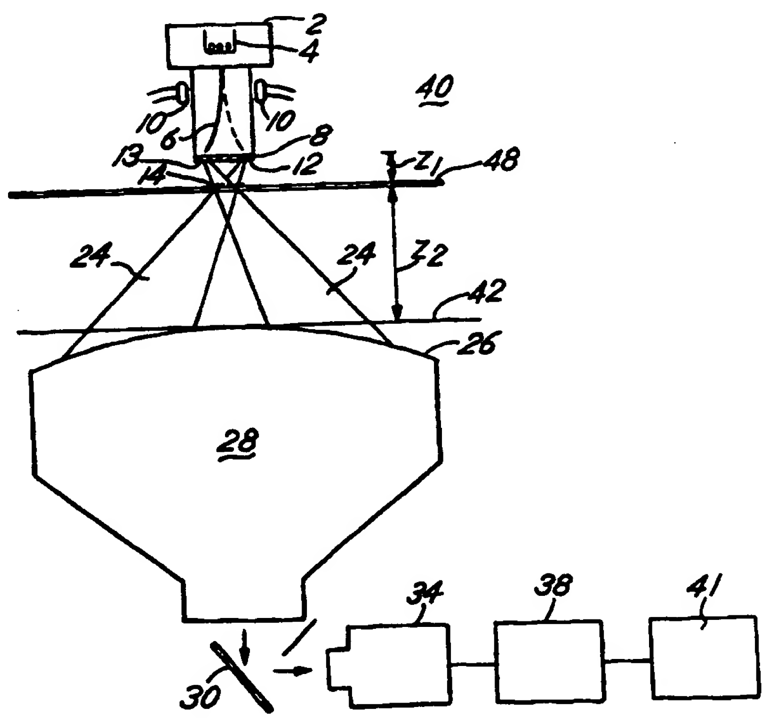

FOR THE PURPOSES OF INFORMATION ONLY

Codes used to identify States party to the PCT on the front pages of pamphlets publishing international applications under the PCT.

AL	Albania	ES	Spain	LS	Lesotho	SI	Slovenia
AM	Armenia	FI	Finland	LT	Lithuania	SK	Slovakia
AT	Austria	FR	France	LU	Luxembourg	SN	Senegal
AU	Australia	GA	Gabon	LV	Latvia	SZ	Swaziland
AZ	Azerbaijan	GB	United Kingdom	MC	Monaco	TD	Chad
BA	Bosnia and Herzegovina	GE	Georgia	MD	Republic of Moldova	TG	Togo
BB	Barbados	GH	Ghana	MG	Madagascar	TJ	Tajikistan
BE	Belgium	GN	Guinea	MK	The former Yugoslav Republic of Macedonia	TM	Turkmenistan
BF	Burkina Faso	GR	Greece	ML	Mali	TR	Turkey
BG	Bulgaria	HU	Hungary	MN	Mongolia	TT	Trinidad and Tobago
BJ	Benin	IE	Ireland	MR	Mauritania	UA	Ukraine
BR	Brazil	IL	Israel	MW	Malawi	UG	Uganda
BY	Belarus	IS	Iceland	MX	Mexico	US	United States of America
CA	Canada	IT	Italy	NE	Niger	UZ	Uzbekistan
CF	Central African Republic	JP	Japan	NL	Netherlands	VN	Viet Nam
CG	Congo	KE	Kenya	NO	Norway	YU	Yugoslavia
CH	Switzerland	KG	Kyrgyzstan	NZ	New Zealand	ZW	Zimbabwe
CI	Côte d'Ivoire	KP	Democratic People's Republic of Korea	PL	Poland		
CM	Cameroon	KR	Republic of Korea	PT	Portugal		
CN	China	KZ	Kazakstan	RO	Romania		
CU	Cuba	LC	Saint Lucia	RU	Russian Federation		
CZ	Czech Republic	LI	Liechtenstein	SD	Sudan		
DE	Germany	LK	Sri Lanka	SE	Sweden		
DK	Denmark	LR	Liberia	SG	Singapore		
EE	Estonia						

METHOD AND APPARATUS FOR IMAGING OBSCURED AREAS OF A TEST OBJECT

RELATED APPLIATIONS:

This application claims the benefit of U.S. Provisional Application No. 60/038,475, filed on February 24, 1997.

BACKGROUND OF THE INVENTION

The present invention relates to imaging inspection systems and techniques. More specifically, the present invention relates to a novel method and apparatus for imaging areas of a test object.

In the field of automatic inspection devices, systems are known that are capable of providing diagnostic information, whether qualitative or quantitative, about a region of interest. In certain applications, such as the inspection of printed circuit boards ("PCBs"), the region of interest may lie in a particular plane within or on the surface of an object being inspected. It is therefore desirable to extract the diagnostic information from the plane containing the region of interest while ignoring information produced by artifacts or substances lying outside the region of interest. The present invention relates to systems and techniques used to produce a representation of a two-dimensional plane passing through a three-dimensional test object.

An automatic inspection device that is capable of providing diagnostic information from the plane containing the region of interest within or on the surface of the test object is shown, for example, in U.S. Patent No. 5,097,492 issued to Baker et al. Baker shows an automated laminography system for the inspection of electronics. An electron beam within an x-ray source is deflected to scan a circular pattern on a target. An x-ray detector is rotated in synchronization with the deflection of the electron beam to intercept x-rays transmitted through the region of interest within the test object. The inspection device produces a laminographic cross-sectional image of a cutting plane.

A disadvantage of the Baker device is that the detector is rotated in synchronization with the steering of the electron beam, requiring precise mechanical control of the detector position as well as increased mechanical complexity. Formation of a high resolution laminographic cross-sectional image depends upon the precise alignment and synchronization of the circular motions of the x-ray source and detector. A further disadvantage of the Baker device is that blurred information may mask diagnostic information, particularly where x-ray

opaque substances are located above or below the region of interest. A still further disadvantage of the Baker device is that the acquisition geometry of the source and detector may not provide a sufficient representation of the region of interest for all PCBs.

Accordingly, it would be desirable to have an improved method and apparatus for imaging obscured devices.

BRIEF DESCRIPTION OF THE DRAWINGS

FIG. 1a is a schematic diagram of an embodiment of an x-ray imaging system in accordance with the presently preferred embodiments;

FIG. 1b is a schematic diagram of a second embodiment of an x-ray imaging system in accordance with the presently preferred embodiments;

FIG. 1c is a schematic diagram of a third embodiment of an x-ray imaging system in accordance with the presently preferred embodiments;

FIG. 2 illustrates an arrangement of image intensifiers for use in the x-ray imaging system shown in FIG. 1c;

FIG. 3 is a schematic diagram of a preferred microfocus x-ray source for use in the x-ray imaging systems shown in FIGS. 1a through 1c;

FIG. 4A is a cross-sectional view of an automated process monitor having an object handling device to be used in conjunction with the x-ray imaging systems of FIGS. 1a-c;

FIGS. 4B through 4G illustrate a sequence of operation for a preferred handling device;

FIG. 5 is a schematic diagram of an embodiment of an angular calibration system according to the presently preferred embodiments;

FIG. 6 is a diagram defining the angular values of an x-ray beam emitted from the x-ray imaging systems of FIGS. 1a-c;

FIG. 7 is an illustration of a portion of a test object having an obscuring body, in which the illustration defines dimensions that may be used in selecting angular values as defined in FIGS. 5 and 6;

FIG. 8 is an illustration of a portion of a test object for further defining dimensions that may be used in selecting angular values in accordance with the presently preferred embodiments;

FIG. 9 is a perspective view of a first plane shown in FIGS. 7 and 8;

FIG. 10 illustrates two solutions in accordance with the presently preferred embodiments for imaging below the horizontal row of obscuring objects shown in FIG. 9;

FIG. 11 illustrates the solutions in accordance with the presently preferred embodiments for imaging below the horizontal and vertical rows of obscuring objects shown in FIG. 9.

FIG. 12 illustrates a collection of transmission images produced from the angular calibration system of FIGS. 5-6;

FIG. 13 illustrates the angular relationship between two dots imaged in one of the transmission images shown in FIG. 12;

FIG. 14 illustrates the x-ray imaging system of FIG. 1a imaging a phantom according to the present embodiment;

FIG. 15 illustrates an embodiment of a phantom to be used according to the presently preferred embodiments;

FIG. 16 illustrates an embodiment of an image processing system to be used according to the presently preferred embodiments;

FIG. 17 illustrates an uncalibrated transmission image taken of the phantom of FIG. 15 according to the presently preferred embodiments;

FIG. 18 illustrates an ideal transmission image of the phantom of FIG. 15 according to the presently preferred embodiments;

FIGS. 19 and 20 illustrate the determination of correction vectors for the transmission images of FIGS. 17 and 18;

FIG. 21 illustrates the correction vectors of FIG. 19 being correlated with a particular image location;

FIG. 22 illustrates the determination of an interpolated correction vector for a pixel;

FIG. 23 illustrates the transmission imaging of a circuit board according to the presently preferred embodiments;

FIG. 24 illustrates four corrected transmission images of the circuit board imaged in FIG. 23;

FIG. 25 illustrates a reconstructed transmission image formed by adding the four transmission images of FIG. 24;

FIG. 26 illustrates a reconstructed transmission image formed by retaining the maximum value of the pixels of the four transmission images of FIG. 24 according to the presently preferred embodiments;

FIG. 27 illustrates a measurement system for determining a coordinate of an object of interest to be used in conjunction with the x-ray imaging systems of FIGS. 1a-c;

FIG. 28 illustrates the transmission image produced from two radiation beams emitted from the measurement system of FIG. 27;

FIG. 29 is an enlarged view of the image plane of FIG. 28;

DETAILED DESCRIPTION OF AN EMBODIMENT OF THE INVENTION

The present invention is best understood upon viewing the embodiments illustrated in FIGS. 1-29, where like elements are denoted by like numerals. FIGS. 1a-c and Fig. 2 each show an x-ray source 2 that preferably incorporates a cathode 4 for producing an electron beam 6. The electron beam 6 is directed toward a transmission target 8 that preferably is made of tungsten. It is understood that other configurations for the x-ray source 2 are possible without falling outside the spirit of the invention, such as having the target 8 be a reflection-type target.

The cathode 4 is supplied with a current of approximately 0.1ma and may have a voltage ranging from -60 kV to -160 kV with respect to the target 8. Preferably, the cathode voltage is computer controlled so that during an inspection cycle the voltage may be optimally adjusted for imaging the region of interest. Generally, the optimum cathode voltage increases with increasing opacity of a test object 14. At the optimum cathode voltage, which is typically approximately -110kV for a PCB, the x-ray source 2 produces an x-ray beam 24 having sufficient energy to penetrate the test object 14 and also having low enough energy so that a resulting image has contrast within the region of interest.

The x-ray source 2 preferably is a microfocus x-ray source in which the electron beam 6 emitted from the cathode 4 is deflected to strike discrete and predetermined focal spot locations 36 on the target 8. Deflection of the electron beam 6 during operation may be accomplished by magnetic coils 10, as shown in FIG. 1a, under local computer control. An example of such an x-ray source 2 is described in U.S. Patent No. 5,020,086, the contents of which are incorporated herein by reference. Alternatively, the electron beam 6 may be deflected electrostatically.

Those skilled in the art of x-ray imaging will appreciate that, rather than deflecting the electron beam 6 in the x-ray source 2, the same effect may be achieved by mechanically moving the x-ray source 2, the test object 14, a detector, such as an image intensifier 28, or a combination of such elements in the imaging chain. For example, rather than deflecting the electron beam 6 to strike a predetermined focal spot locations on the target 8, the entire x-ray source 2 may be laterally displaced an equivalent distance, thereby altering the spatial relationship between the x-ray source 2 and a region of interest within the test object 14 in the desired manner. Likewise, the test object 14 may be moved to a number of predetermined locations while the x-ray source 2 remains stationary. As a further example, the detector may be physically displaced, such as by rotating the detector about the region of interest to a

predetermined number of discrete points. As a still further example, the x-ray source 2 and the detector may both be moved in relation to the position of the test object 14. Each of these examples allows a series of transmission x-ray images to be formed as the arrangement of the x-ray source 2, the test object 14 and the detector varies in a discrete, as opposed to continuous, manner.

Figure 3 is a schematic diagram of a preferred two-stage microfocus x-ray source 2. Within the x-ray source 2, an electron beam 6 is emitted by a cathode filament 52 through an aperture 54 in a bias cap 56. The electron beam 6 is directed toward a target 8 from the filament 52. The electron beam 6 is aligned by x_1/y_1 deflection coils 60 and then passes through a measuring aperture 62 and a condensor coil 64. The electron beam 6 is again aligned by x_2/y_2 deflection coils 66, after which it passes through an objective focus coil 68 and an objective aperture 70. A steering coil 72 is disposed between the objective aperture 70 and the target 8. The steering coil 72, under microprocessor control (not shown) may cause the electron beam 6 to be deflected to strike discrete and predetermined focal spot locations 36 on the target 8.

The x-rays emitted from the target 8 pass through a window 12 made of an x-ray transparent material such as Beryllium and/or through an x-ray spectrum filter (not shown). The x-ray spectrum filter may be chosen to modify the x-ray energy spectrum in such a way that adjusts the sensitivity of the system to the component under inspection. In addition, an electrically actuated mechanical shutter (not shown) may be provided to contain the emitted x-rays without interrupting power to the x-ray source 2. Note that the shutter may be moved pneumatically in response to an electrical signal from a solenoid.

As shown in FIGS. 1a, 1b and 1c, the x-rays generated by source 2 are directed toward the test object 14. Though the choice of the test object 14 is arbitrary, for the presently preferred embodiments the test object 14 preferably comprises either an electronic assembly or a circuit board including electronic components electrically connected to the circuit board through solder joints. The presently preferred embodiments allow one to identify defects in circuit boards, for example as disclosed in U.S. Patent No. 4,809,308, whose entire contents are incorporated herein by reference.

A handling system may be provided to automatically load test objects to, and unload test objects from, the x-ray imaging systems shown in FIGS. 1a through 1c. As schematically shown in FIG. 4A, an inlet conveyor 16 transports the test object 14 from an outside factory conveyor (not shown) to an X-Y table 18 in an inspection chamber 19. Once the X-Y table 18 has received the test object 14, the x-ray imaging inspection cycle can begin while the outlet

conveyor 20 transports the previously inspected test object to the factory and the inlet conveyor 16 retrieves the next test object. A handling system for transporting a device to or from a radiation chamber is described in U.S. Patent No. 5,491,737, the contents of which are incorporated herein by reference.

Figures 4B through 4G illustrate a sequence of operation for a preferred handling system. Figures 4B through 4G are sectional views of a shuttle assembly 74. In accordance with a preferred embodiment, a first shuttle assembly 74 contains the inlet conveyor 16, shown in Figure 4A, and a second shuttle assembly 74 contains the outlet conveyor 20, shown in Figure 4A. Thus, the preferred inspection apparatus will have two shuttle assemblies 74; one located adjacent to the input to the inspection chamber 19 and one located adjacent to the output of the inspection chamber 19.

As shown in Figures 4B through 4G, the shuttle assembly 74 includes a shuttle conveyor 76, which is aligned with opposed openings 78 and 80. A pivotable radiation guard 82 is located within the shuttle assembly 74. The radiation guard 82 preferable has opposing curved walls 84 and 86.

Preferably, the shuttle assembly 74 and the radiation guard 82 are constructed from sheet steel. In addition, those portions of the inspection apparatus and the shuttle assembly 74 that are within the direct line of sight of the x-ray source 2, including the curved walls 84 and 86, are preferably lined with 1/16"- 3/16" thick lead sheets.

The operational sequence illustrated in Figures 4B through 4G will now be described with reference to the shuttle assembly 74 that is located adjacent to the input of the inspection chamber 19. Of course, this description also applies to the shuttle assembly 74 located adjacent to the output of the inspection chamber 19, except that the position of the factory conveyor 88 and the x-y table 18 would be switched.

As shown in Figure 4B, the radiation guard 82 is pivoted away from the opening 80, while blocking the opening 78. The shuttle conveyor 76 is extended through the opening 80, where it meets the factory conveyor 88. This is the loading position of the input shuttle assembly 74. In this position, a circuit board, such as the board 14, may be transferred from the conveyor 88 to the shuttle conveyor 76.

In Figure 4C, the shuttle conveyor 76 is retracted into a centered position within the shuttle assembly 74. After the shuttle conveyor 76 is retracted, the radiation guard returns to its level position, in which the curved walls 84 and 86 block the opposed openings 78 and 80, as shown in Figure 4D.

In Figure 4E, the radiation guard 82 has pivoted away from the opening 78, while the wall 86 continues to block the opening 80. Next, the shuttle conveyor 76 is extended through the opening 78, where it meets with the x-y table 18, as shown in Figure 4F. This is the unloading position of the input shuttle assembly 74. In this position, a circuit board, such the test object 14, may be transferred from the shuttle conveyor 76 to the x-y table 18. Once the transfer is complete, the shuttle conveyor 76 is retracted and the radiation guard returns to its level position, as shown in Figure 4G.

The shuttle conveyor 76 preferably includes a board stop, which operates to stop the shuttle conveyor 76 when the test object 14 is properly positioned thereon. A mechanical board stop is described in U.S. Patent No. 5,491,737. Two such board stops may be used on the shuttle assembly 74, with the board stops being positioned to prevent the test object 14 from rotating when the test object 14 strikes the board stops. Preferably, an electronic board stop is utilized so that the test object 14 is not jarred or displaced on the shuttle conveyor 76. The electronic board stop may be, for example, an optical sensor that is located to produce a signal to stop the shuttle conveyor 76 when the test object 14 reaches the appropriate position within the shuttle assembly 74.

It is expressly envisioned that the shuttle assembly 74 may be of appropriate dimensions to accommodate more than one test object 14 simultaneously. For example, the shuttle conveyor 76 may receive two test objects from the conveyor 88 at the same time. The two test objects may then be simultaneously unloaded onto the x-y table 18.

When the test object 14 is mounted on the X-Y table 18, the test object 14 may be translationally moved along the x and y directions so that an area of interest, such as a solder joint, can be imaged. In addition, as represented by the vertical arrows in Figure 4A, the x-ray source 2 and the detector 26, 28 may move along the z axis, as is further described below.

Once the test object 14 is properly positioned, a beam of radiation, such as the x-ray beam 24, is projected toward, for example, a solder joint or a component on the test object 14. The x-ray beam 24 originates from the appropriate predetermined location 36 on the target 8 of the x-ray source 2. A portion of the x-ray beam 24 is transmitted through and modulated by the test object 14, after which the x-ray beam 24 strikes a detector that is capable of producing an x-ray shadowgraph containing the modulation information from the test object. An example of such a detector is a fluorescent or scintillating screen 26 supported by an image intensifier 28. Alternatively, the detector may be a high resolution scintillating screen, such as a Cesium-Iodide scintillating screen, in which case the image intensifier 28 may not be required.

As shown in FIG. 1a, the image intensifier 28 is positioned in-line with the x-ray beam 24. It is not necessary that the x-ray source 2 be located above the test object 15 and the detector therebelow, as shown in the accompanying figures. It is the alignment of the source, test object and detector with respect to the x-ray beam that is important. In fact, for applications that do not require the use of the image intensifier 28, an inverted geometry is preferred.

The x-rays striking the fluorescent or scintillating screen 26 produce a visible light, shadowgraph or transmission image of the volume of the object 14 that falls within the x-ray beam 24. If the detector includes an image intensifier 28, as shown in FIGS. 1a through 1c and 2, the visible image at the output of the image intensifier is amplified in brightness.

The image intensifier 28 in the embodiments of FIGS. 1a-c, 2 and 3 is positioned to receive the x-rays that are transmitted through the test object 14. The face plate of the image intensifier 28 is preferably formed by the fluorescent or scintillating screen 26, which converts x-rays to visible light. The screen 26, which is typically curved or spherically shaped, captures individual shadowgraph images that are viewed by a camera 34, such as a CCD camera, and subsequently digitized by the image processor 38. The image intensifier 28 provides high conversion efficiency resulting in improved signal-to-noise ratio over typical passive screen-based conversion systems. High resolution scintillating screens also provide improved performance in comparison to the typical passive screen-based conversion systems. These features permit optimizing the field-of-view, resolution, and throughput for virtually any board type, even if the board has a wide variation of component pitch.

The use of a large format imaging system, such as the image intensifier 28, shown in FIGS. 1a-b, eliminates the need to have a spinning detector, reducing the mechanical complexity of the system and improving system reliability and the repeatability of results. This approach simplifies the mechanical requirements for the image collection system and allows static rather than dynamic image train alignment and calibration. Distortion in the visible light images that may be produced when the images are projected toward the outer circumference of the curved or spherical screen 26 on the image intensifier 28 may be corrected as described below.

The x-ray source 2 and the image intensifier 28 are mounted on independent vertical drive mechanisms allowing a continuously variable field-of-view, ranging from approximately 0.1" to approximately 1.0", to be obtained. In particular, the x-ray source 2 is mounted on a programmable Z-axis, which changes the distance between the target 8 and a plane 48 containing the region of interest within or on the surface of the test object 14. The

distance between the x-ray source 2 and the plane 48 is referred to herein as Z_1. The image intensifier 28 is also mounted on a programmable Z-axis, which changes the distance between the object plane 48 and the screen 26. The distance between the plane 48 and the screen 26 is referred to herein as Z_2. Variation of the field of view may be accomplished by varying either or both of the distances Z_1 and Z_2. The imaging system described herein may be calibrated along the Z-axis as disclosed in U.S. Patent No. 5,500,886, the contents of which are incorporated herein by reference, to provide an improved representation of the region of interest.

The visible light image produced by the screen 26 and the image intensifier 28 may be reflected by an optical system. In FIG. 1b, a preferred optical system is shown. The optical system includes a computer-controlled view selector 31, which improves the resolution of the system. During image collection, the view selector 31 is synchronized with the movement of the x-ray focal spot to the predetermined locations 36 to provide a selected portion of the visible light image from the screen 26 of the image intensifier 28 to the camera 34. The camera 34 typically is capable of providing a 512 x 512 pixel video image. Because the view selector 31 provides only the selected portion of the entire image intensifier surface to the camera 34, the resolution of the image system is increased.

As shown in FIG. 1b, the view selector 31 preferably contains two independently rotatable mirrors 33 and 35, the first mirror 33 being rotatable so as to vary the location of the selected portion of the image intensifier surface along the X-axis. The second mirror 35 is rotatable so as to vary the location of the selected portion of the surface along the y-axis. The mirrors 33 and 35 may be controlled by a computer 38 so that the image reflected from the mirrors is received by camera 34, in which case the computer 38 may also control the deflection of the electron beam 6 in synchronization with the movement of the mirrors 33 and 35 and the cathode voltage.

Alternatively, the optical system may be a planar mirror 30 having an aluminized front surface, as shown in FIG. 1a. The mirror 30 may be mounted at an angle of 45 degrees to the horizontal to reflect the visible light image from the image intensifier 28 through 90 degrees. The visible light image is amplified in brightness by the image intensifier 28 and is then reflected at a 90 degree angle by the mirror 30 to a lens 32 mounted upon a video camera 34. The mirror 30 allows the camera 34 to be positioned outside the path of the x-ray beam 24 when a non-x-ray-opaque detector is used or to conserve vertical space. The mirror 30 is not required if the detector is opaque to x-rays or if the camera 34 is not sensitive to x-rays.

In an alternative embodiment, the large format image intensifier 28 is replaced by multiple small-format image intensifiers. In FIGS. 1c and 2, an arrangement of nine small-format image intensifiers is illustrated. A camera 34 may be used for each of the multiple small-format image intensifiers, in which case the view selector 31 including the rotating mirrors 33 and 35 is unnecessary.

Like the large format image intensifier 28, the arrangement of small-format image intensifiers eliminates the need to have a spinning detector and allows static rather than dynamic image train alignment and calibration. A benefit provided by the small-format image intensifiers is that, because the curved or spherical screen 26 is much smaller, the small-format image intensifier produces less distortion when a visible light image is projected toward its outer circumference. However, the arrangement of small-format image intensifiers may limit the selection of the predetermined locations 36.

A single camera 34 in conjunction with a view selector, such as the view selector 31, and a bundle of fiber optic cables may alternatively be used with the arrangement of small-format image intensifiers. For each of the small-format image intensifiers, a fiber optic cable may couple the visible light image from the image intensifier to the view selector 31.

A commercially available CCD camera that is suitable for these applications is available from Cohu, Inc. of San Diego, California as Model No. 4915. It is envisioned that, as CCD camera technology develops, a CCD camera that is capable of providing approximately 3000 x 3000 pixel resolution will become available. If such a CCD camera were used with the large format image intensifier 28 the view selector 31 would no longer be required, as the CCD camera would be capable of viewing the entire screen 26 on the image intensifier 28 while providing equivalent resolution to the currently available 512 x 512 pixel CCD cameras. In the same manner, a single 3000 x 3000 pixel CCD camera could be used to view the multiple small-format image intensifiers by using fiber optic cables to transmit the visible light images from the small-format image intensifiers to the CCD camera. Moreover, if the inverted geometry described above is utilized, a small high resolution scintillating screen may be viewed by a CCD camera providing approximately 1000 x 1000 pixel resolution. Quite apart from obviating the need for the view selector 31, the use of a high resolution CCD camera is therefore also an alternative to an embodiment having a physically movable detector, since image processing and image formation functions may be performed on only a portion of the CCD image by selecting the appropriate pixels from a subregion of the entire CCD image.

The analog output of CCD camera 34 is provided to image processing/defect recognition system 38 which processes data derived from the transmission image to formulate an image on a display, such as a video monitor 41, or to provide a printed defect analysis, as descried in U.S. Patent No. 4,809,308. The image processing/defect recognition system may also provide feedback for process control.

Another function performed by image processing system 38 is to calibrate the imaging system prior to imaging a region of interest, such as a solder joint. In particular, an angular calibration system 40 accurately determines the angular direction θ of the x-ray beam 24. The preferred angular calibration system is shown in U.S. Patent No. 5,500,886, which is entitled "X-ray Position Measuring and Calibration Device" and whose entire contents are incorporated herein by reference. It is to be understood that other calibration systems may be used without departing from the spirit of the present invention, as long as the angle θ may be accurately determined.

The angular calibration system 40 utilizes the x-ray imaging system described previously and shown in FIGS. 1a-c and 2 to accurately determine the angle θ FIG. 5 illustrates a portion of the calibration system 40 in greater detail. A radiation source, such as the x-ray source 2, is located along a first direction, such as the z-axis. As described in U.S. Patent No. 5,500,886, the radiation source 2 generates a beam of radiation, such as x-ray beam 24, where the beam axis 25 is directed along an inclinational angular direction θ measured with respect to the z-axis. Furthermore, when viewed along the z-axis, the beam axis 25 of the x-ray beam 24 strikes an image plane 42 at an azimuthal angle φ with respect to the x-axis, as shown in FIG. 6. It should further be noted for purposes of the presently preferred embodiments that the inclinational angular direction θ may also be represented by the components θ_x and θ_y, rather than the angles θ and φ, by transforming the angles θ and φ from polar to cartesian coordinates. The angles θ and φ, and any components thereof, are measured with respect to the beam axis 25, as shown in FIGS. 5 and 6.

The angular calibration system 40, as described in pending U.S. Patent No. 5,500,886, allows the inclinational angular direction θ to be accurately determined for an x-ray beam generated from any predetermined location 36 of the electron beam focal spot on the target 8. During a board inspection cycle, shadowgraph images are projected toward specific locations on the surface 26 of the image intensifier 28 by moving the electron beam 6 to a set of predetermined focal spot locations 36 on the target 8. Once the electron beam 6 strikes the target 8 at one of the predetermined focal spot locations 36, an x-ray beam 24 is emitted

toward the object 14. For a given predetermined location 36, the emitted x-ray beam 24 will be directed toward the object 14 at a given inclinational angular direction θ, which, as described above, may be described by its orthogonal components θ_x and θ_y. Accordingly, a source image 49 will be formed at the screen 26 for each of the predetermined locations 36.

As discussed above, U.S. Patent No. 5,097,492 shows an electron beam within an x-ray source is deflected to scan a continuous circular pattern on a target. The detector also rotates in a circular pattern. U.S. Patent No. 5,020,086 describes an imaging system in which a series of images are obtained by scanning an electron beam stepwise through a circular pattern about a central axis. The series of images are then combined to form a representation of a region of interest. Without knowledge of the geometry of the body or bodies obscuring the region of interest, the circular scanning pattern may be assumed to provide an acceptable representation of the region of interest. In accordance with the presently preferred embodiments, however, information about the geometry of the obscuring body or bodies may be used to provide an improved representation of the region of interest.

In accordance with a presently preferred embodiment, the imaging geometry used to produce the representation of the two-dimensional plane may be optimized for a particular test object to reduce the data required to produce the two-dimensional representation and to minimize the effects in the representation of substances located above or below the desired two-dimensional plane. The imaging geometry, as used herein, refers to the pattern of the predetermined locations 36 on the target 8, and the corresponding inclinational angular direction θ of the resulting x-ray beam 24.

Referring now to FIG. 7, a portion of a test object 56 is shown. The test object includes a first plane 58 and a second plane 60. The first plane 58 is positioned nearer to the x-ray source 2 than is the second plane 60, and the first plane 58 is separated from the second plane 60 by a distance *t*. The distance *t* is measured along the Z-axis with the intersection of the Z-axis with the plane 60 defining the origin. Accordingly, if the second plane 60 was located above the first plane 58, then the value of *t* would be negative. An x-ray opaque body 62 having a width *w* is located about the first plane 58. In the example of FIG. 7, the second plane 60 defines the region of interest within the test object 56.

Although the body is described as being opaque, it is to be understood that it is not necessary that the body completely block the transmission of x-rays. Rather, as used herein, an opaque body is a body that attenuates x-rays to a greater extent than the material surrounding the body. The three-dimensional construction of a PCB-mounted solder

connection is nearly binary in x-ray attenuation characteristics. Each volume element (voxel) can be modeled as being entirely filled with either metal (i.e., solder or metal wire), or a low x-ray attenuation material (i.e., air, plastic, organic material, etc.).

In order to obtain an unobstructed representation of the second plane 60, the electron beam 6 within the x-ray source 2 must be deflected to more than one predetermined location 36, creating corresponding source images for each predetermined location. There will be a minimum number of predetermined locations 36 that are required so that every part of the region of interest, in this example the second plane 60, may be imaged without obstruction by the body 62 in at least one of the source images.

Referring again to FIG. 7, a point C is illustrated in the second plane 60. The point C is located within the second plane 60 at the distance t below the midpoint $w/2$ of the body 62. To obtain an unobstructed image of the point C, the x-ray beam 24 must be generated from an appropriate predetermined location 36 such that the x-ray beam 24 passes beside rather than through the body 62. As shown in FIG. 7, the minimum angle of x-ray beam inclination that satisfies this requirement is:

$$\theta_{max}=\arctan(w/2t) \qquad (1)$$

An unobstructed image of points A and B within the second plane 60 may be obtained from inclination angles of θ_{max} or less, while an unobstructed image of points D and E may be obtained from inclination angles between 0 and $-\theta_{max}$. Accordingly, the smallest range of inclination angle values that may be used to obtain an unobstructed representation of the second plane 60 is given by:

$$-\theta_{max} \leq \theta \leq \theta_{max} \qquad (2)$$

Generally, it is preferable to utilize the minimum number of images that will provide an unobstructed view of the region of interest. An unobstructed representation of the second plane 60, including points A through E, may be obtained from two images, a first image obtained at the inclination angle of $-\theta$ and a second image obtained at the inclination angle of θ. As may be seen from FIG. 7, $+\theta$ and $-\theta$ are the minimum angles of inclination for an unobstructed representation of the second plane 60. Larger angles may alternatively be used and it is not necessary that the positive and negative (+ and -) angles be of the same magnitude.

FIG. 8 is a cross-sectional view of a test object, which is like the test object shown in FIG. 7 except that additional bodies, such as the bodies 63 and 64 are disposed about the first plane 58. The minimum separation between any two adjacent bodies is the distance s_{min}. For

purposes of the following analysis, it is assumed that the distances s_{min} and w are small with respect to distance Z_1. An unobscured representation of the second plane 60 may be obtained by using the separation of distance s_{min} between adjacent bodies as a "window" to the region of interest. In accordance with a presently preferred embodiment, the inclination angle may be incremented to "walk" the view within the window across the region of interest.

The movement of each view through a given window resulting from a change in angle $\Delta\theta$ will be $t \times \tan(\Delta\theta)$, for small angles θ. In order that the views overlap, it is necessary that $t \times \tan(\Delta\theta) \leq s_{min}$, which therefore limits the angular increment $\Delta\theta$ to $\Delta\theta \leq \arctan(s_{min}/t)$.

In the example described with respect to FIG. 7, it was shown that two images obtained by angles of inclination separated by $2\theta_{max}$ provided an unobscured representation of the region of interest, i.e., the second plane 60. Where the test object includes an arrangement of bodies, as shown in FIG. 8, an unobscured representation of the region of interest may be obtained from a series of images in which the inclination angle is incremented by $\Delta\theta$ across the range of $2\theta_{max}$.

For an arrangement of bodies as shown in FIG. 8, θ_{max} as given by equation 1 is calculated from the maximum width w_{max} associated with the bodies. In the case of the bodies being periodically disposed about the plane 58, the dimensions s and w will be constants. The body 62 in FIG. 8 has the maximum width. The total number of images required is:

$$n=[2\theta_{max}/\Delta\theta] \qquad (3)$$

which is preferably rounded up to the next integer. Preferably, the overlap of the views of the second plane 60 are evenly distributed by using the integer value n to recalculate the incremental angle, $\Delta\theta$ as follows:

$$\Delta\theta=2\theta_{max}/n_{integer} \qquad (4)$$

The above discussion assumes that a given $\Delta\theta$ will produce a given movement of the unobscured view across the second plane 60. This assumption is only true for small values of θ. An alternative approach that is not constrained to small values of θ is to allow the position of the view to move in evenly sized steps across the second plane 60 and to compute the angle θ corresponding to each such position. If the variable view position is measured in respect to the view position when $\theta = 0$, then the view must take positions from $-\frac{w}{2}$ to $+\frac{w}{2}$. The number of steps will be $n = w/s_{min}$, which is rounded to the next highest integer. The positions of the view will therefore be:

$$Pi = -\frac{w}{2} + i\frac{w}{n}, \qquad (5)$$

where i varies from 1 to n. The corresponding angles θ_i are:

$$\theta_i = \tan^{-1}\left(\frac{Pi}{t}\right). \qquad (6)$$

This general formulation will produce an efficient set of inclinational angular directions θ for all obscuring geometries. However, in some cases, an equivalent quality representation of the plane 60 may be produced from a smaller set of inclinational angular directions, depending on the particular geometry of the obscuring bodies on or within the test object.

If the obscuring bodies have a vertical dimension h that is significant in comparison to the separation s between the bodies, then the above calculations must be modified to account for the corresponding effective reduction in size of the separation s. At a given angleθ, $s_{effective} = s - h\ tan(\theta)$. In this case, the above θ_i calculation may be repeated with the steps made smaller to account for the smaller $s_{effective}$ as a function of the angle θ.

The predetermined locations 36 of the electron beam focal spot on the target 8 for imaging the test objects in FIGS. 7 and 8 lie along a line that is parallel to the bottom of the page on which the figure is shown. Some test objects may, however, present a more advantageous imaging geometry in another direction. For example, a test object as shown in FIG. 8 may have the bodies arranged in another direction in which the width w of the bodies is smaller and/or the separation s between the bodies is greater in another direction. In this case, it is preferable to direct the focal spot to predetermined locations 36 along a line in that direction because fewer images are required to provide an unobstructed view of the region of interest.

In an alternative arrangement of the test object, different features may be analyzed along differing directions, producing differing sets of the required θ components in each direction. The region of interest may then be represented for a given obscuring geometry by using a set of θ and ϕ values that includes all of the required θ components.

For example, one specific case of an obscuring geometry is given by the horizontal row of obscuring objects 70 in FIG. 9. Since the obscuring objects 70 are thinner (smaller w) in the horizontal direction, the analysis should be performed in that direction, producing required angular components in that direction (θ_x). From the above analysis,

$$\theta_x = \tan^{-1}\left(\frac{W_x}{2t}\right),\ and\ \Delta\theta_x \leq \tan^{-1}\left(\frac{S_x}{t}\right). \quad (7)$$

The above analysis does not specify the y-component of the angles. These can be chosen on any convenient basis. Obvious choices are $\theta_y = 0$, resulting in a linear "scan," or setting θ_y to the maximum available angle. This latter choice is especially useful if more than the minimum number of viewing angles are to be used. In this case, θ_y can take values of plus and minus the maximum available angle, thus providing flexibility to account for obscuring features not accounted for in the basic analysis (e.g., lead frames, ground planes, etc.).

FIG. 10 shows these possible options for imaging the horizontal row. In this plot, points are plotted in x and y according to their θ_x and θ_y components. The plotted points represent the selected predetermined locations 36 on the target 8. The plotted points, "x", represent the linear scan solution, i.e., $\theta_y = 0$. The plotted points, "•", represent the solution in which θ_y is set to plus and minus (+ and -) the maximum available angle. The predetermined locations 36 represented by θ_x and θ_y may alternatively be represented in terms of the θ and ϕ values described above by the equations:

$$\theta = \sqrt{\theta_x^2 + \theta_y^2}\ and\ \phi = \tan^{-1}\left(\frac{\theta_y}{\theta_x}\right), \quad (8)$$

which describe the usual cartesian-to-polar coordinate transformation.

The analysis can be expanded to include the vertical row of features in FIG. 9. FIG. 9 is a perspective view of the plane 58 taken along the Z-axis, i.e., the plane 58 lies in the x-y plane. For these features, the analysis is best done in terms of θ_y, since their vertical dimension is smaller. Combining this analysis for θ_y with the θ_x results above places conditions on both θ_x and θ_y:

$$\theta_{x\,max} = \tan^{-1}\left(\frac{W_x}{2t}\right),\ \Delta\theta_x \leq \tan^{-1}\left(\frac{S_x}{t}\right) \quad (9)$$

$$\theta_{y\,max} = \tan^{-1}\left(\frac{W_y}{2t}\right),\ \Delta\theta_y \leq \tan^{-1}\left(\frac{S_y}{t}\right). \quad (10)$$

FIG. 11 shows two of the many options for meeting these conditions. A first solution is represented by the plotted points, "x", and a second solution is represented by the plotted points, "•".

Although the obscuring objects shown in FIGS. 7-9 are arranged about a plane located above the plane containing the region of interest, it is to be understood that the present

invention is not limited to this arrangement. The region of interest may lie on the surface of the test object or in any plane within the test object. For example, when the plane 60 containing the region of interest is located above the plane 58 containing the obscuring bodies, the value of the distance *t* will be negative in the above equations. Therefore, for any location of the region of interest, a presently preferred embodiment provides predetermined locations 36 for obtaining an unobscured representation of the region of interest.

Accordingly, by using an imaging geometry that is not constrained to a circular pattern, an improved representation of a region of interest may be obtained. In the instance where the test object 14 is a PCB, the flexibility of defining the pattern of predetermined locations 36 on the target 8 according to the geometry of the obscuring body or bodies improves the quality of the representation of the region of interest, while decreasing inspection times. On a PCB, surface mounted devices frequently obscure the regions above or below the devices. Many of these devices have a square or rectangular geometry so that the regions above or below these devices are best represented by using a non-circular scanning geometry, as described above. In addition, many of these devices have a periodic arrangement of leads that may obscure regions above or below the device. Of course, where the device geometry is circularly symmetric, such as where the devices are ball grid arrays or flip-chip attach arrays, the presently preferred embodiments may utilize a circular scan geometry to obtain the best representation of a region below the devices. It should be noted that, as PCB device geometries change with future developments, the presently preferred embodiments provide a means to select the optimum imaging geometry. Moreover, it is to be understood that the above-described determination of the optimum imaging geometry may be applied to test objects other than PCBs.

In accordance with the presently preferred embodiments, apparatus is, therefore, provided for producing an unobscured representation of a region of interest. In addition, the presently preferred emboidments provide a method of selecting the discrete predetermined locations 36 in order to efficiently and effectively produce an unobscured representation of the region of interest.

It is envisioned that the present invention may be used in conjunction with an apparatus and method for forming a reconstructed transmission image as described below. Rather than simply summing eight corresponding pixels from eight source images to form a single pixel in the reconstructed image, the apparatus and method described below combines the pixels in a non-linear manner. The method and apparatus described above may be utilized to provide unobscured source images, which may result in an improved reconstructed image.

Referring again to Figures 5 and 6, accurate measurement of the angles θ and ϕ is important when one reconstructs a tomographic image of an object from a plurality of images formed from x-ray beams 24 emanating from different directions. Measurement of the angular direction of the x-ray beam 24 may be accomplished by placing two reference elements 44, 46, for example, near the object plane 48. The reference elements 44, 46 preferably are made of an x-ray absorbent material, such as lead, and are spherical in shape so that any distortion in their image is equal in all directions. The reference elements 44, 46 may be present on a circuit board 14 to be imaged or positioned within a block of x-ray transparent material, such as plastic. The two reference elements 44, 46 are preferably positioned at the same x and y coordinates but are separated from each other along the z-direction by a predetermined distance H, such as 40 mils.

It is understood that other calibration tools may be used without departing from the spirit of the present invention. For example, the reference elements 44 and 46 may be positioned at different x and y coordinates. However, the calculations involved are more complicated than when the elements 44 and 46 are aligned along the z-direction. In another embodiment, a single reference element 44 is moved to two Z-axis calibration positions separated by distance H by a movement device, such as moving the x-ray source 2 and image intensifier 28 both by a distance H so that the sum $Z_1 + Z_2$ is unchanged. An image is taken at each calibration position. The two images are overlaid resulting in an image that corresponds to the image of two reference elements 44, 46 located at the two calibration positions.

In each of the embodiments described above, the reference elements are positioned by the X-Y table 18 so that they are located under the center of the target 8 and are located near the object plane 48. Besides H, the distance Z_1 between the x-ray source 2, 36 and object plane 48 and the distance Z_2 between the object plane 48 and the image detector, such as image intensifier 28, are also known.

Once the reference elements 44, 46 are properly positioned, a first x-ray beam 24 is emitted by the x-ray source 2 so that a first image of both reference elements 44, 46 is generated. The first x-ray beam 24 is emitted along a direction that is to be used for forming an image of an object of interest. As shown in FIG. 12, multiple transmission images I_i (i=1, 2...8) of the reference elements are taken along those directions corresponding to the beam directions for imaging the object of interest. Note than an image taken along the z-axis, θ=0 may be taken as well.

As seen by the enlarged view of I_2 shown in FIG. 13, each transmission image of the reference elements 44, 46 comprises two dots 50, 52, respectively. The separation vector R between the two dots 50, 52 changes in magnitude, R and direction γ depending on the image selected. R and γ can be measured manually or by a microprocessor, wherein γ corresponds to the angel ϕ of the x-ray beam. The microprocessor then can calculate the inclination angle θ based on the values of R and H by use of the equation:

$\theta_{Ii} = \tan^{-1}[(R_{i1}-R_{i2})/H - (R_{i1} + R_{i2})/Z_1]$, where R_{i1} and R_{i2} are the signed displacements of the dots 50, 52 measured from a point 53 where beam axis 25 intersects the ith digitized image. They are measured in units of distance in the imaging plane 42. Note that if one reference element lies exactly along beam axis 25 then $R_{i2} = 0$ and R_{i1} equals the distance, R, between the two images and $\theta_{Ii}= \tan^{-1}[R/H - R/Z_1]$.

A calibration data acquisition system 54 according to a presently preferred embodiment may be used separately or in conjunction with the angular calibration system 40 described above. As shown in FIG. 14, the calibration data acquisition system 54 employs the x-ray imaging system of FIG. 1a to image a phantom 56 positioned at a fixed position in space, preferably approximately 1 cm from the x-ray focal spot. It is understood that system 54 may be used in conjunction with the x-ray imaging system of FIG. 1b.

The phantom 56 comprises a plane of radiant energy absorbing reference elements 58 at calibrated spatial locations. Each of these energy absorbing elements 58 will be referred to as a dot and the plane of the dots will be referred to as the object plane. For example, the phantom 56 may comprise a planar grid of uniformly spaced metal dots 58 attached to an x-ray transparent carrier as shown in FIG. 15. In another embodiment, the phantom 56 consists of a printed circuit board with a rectangular array of round copper discs or dots etched onto the surface. In one embodiment, these copper dots measure 5 mils in diameter, 1 mil in thickness, and are located on 20 mil centers in both the x and y directions. Metallic lead is plated onto the surface of the dots to increase the x-ray opacity.

Once the phantom 56 is positioned, the x-ray focal spot is sequentially positioned to a plurality of predetermined focal spot positions 36 (preferably eight) on the target 8. At each focal spot position 36, x-ray beam 24 passes through the phantom 56 at a distinct angle. For each distinct angle, an x-ray beam 24 strikes the dots 58 and produces a calibrated image I_c on an image detector, such as image intensifier 28.

As shown in FIG. 16, the optical output image from the image intensifier 28 is viewed by a camera 34, either directly or through one or more mirrors 30. The image received by the

camera 34 is then converted to a digital signal representing the collected image by analog-to-digital converter 60. The digital representation for each distinct angle is then stored in a memory of a digital computer to be later processed.

As shown in FIG. 17, the locations of the images or projections 62 of the dots 58 are not uniformly spaced for each stored calibration image I_{ic} (i=number of stored calibration image). The lack of spatial uniformity is due to the "pincushion" effect and other distortions in the image intensifier. A computer algorithm identifies the location r_{in} (n=number of dot; i=number of ideal calibration image) of the centroid of each of these dot projections 62 in terms of image row and column number. The location of the centroid is referred to as the measured location.

The computer algorithm also identifies for each image an ideal representation location R_{in} (n=number of dot, i=number of ideal calibration image) associated with each dot. This calibration location Rinconsists of the row and column that the dot 58 would appear in an ideal image I_{ic} (i=number of ideal image) of the phantom 56 and does not rely on measured data, but rather on the known construction of the phantom 56. FIG. 18 shows the calibration locations R_{in} of dots 58 when arranged in a square grid; just as the calibration phantom would appear if there were no distortion in the imaging system.

As shown in FIGS. 19 and 20, the computer algorithm then calculates a calibration vector $C_{in} = R_{in} - r_{in}$, i.e. the number of rows and columns that the measured location r_{in} must be shifted by to move it to the ideal representation location R_{in}. This calibration vector C_{in} is stored in the computer's memory as being associated or correlated with the ideal representation location R_{in}. The storage and correlation of C_{in} is schematically shown in FIG. 21.

An interpolated calibration vector V is then calculated for each pixel in each of the calibration images. These vectors are interpolated and extrapolated from the calibration vectors C_{in}. This set of interpolated calibration vectors is stored in the computer's memory. An example of calculating an interpolated calibration vector V is shown in FIG. 22, where the interpolated calibration vector V at any location in the image can be calculated as an interpolation of the four surrounding calibration vectors C_{in}. For example, the interpolated calibration vector V_E at location E can directly be calculated as a linear interpolation of the calibration vectors C_A, C_B at locations A and B. Likewise, the interpolated calibration vector V_F associated with location F can be directly calculated as a linear interpolation of the calibration vectors C_C, C_D at locations C and D. The interpolated calibration vector V_G at an arbitrary location, such as G, can then be found by linear interpolation from the interpolated

calibration vectors V_E, V_F at E and F. In this manner, an interpolated calibration vector V (r_j) (r_j = location of jth pixel) can be calculated and stored for each pixel in each of the eight calibration images.

An example of calculating an interpolated calibration image is as follows: Let α represent the fraction of the distance that location E is between locations A and B. In other words, α is equal to the distance between locations A and E divided by the distance between locations A and B. The X and Y components of the interpolated calibration vector V_E are then determined from the equations:

$$V_{EX}=\alpha\, C_{BX} + (1-\alpha)\, C_{AX}$$

$$V_{EY}=\alpha\, C_{BY} + (1-\alpha)\, C_{AY},$$

where the subscripts X and Y refer to the x and y components of the referenced vector. V_F is calculated in a similar manner. From the method shown above, the interpolated calibration vector can be found on a straight line between any two calibration vector locations. Likewise, the interpolated calibration vector, at an arbitrary location, such as G, can be found by linear interpolation from previously calculated vectors, such as V_E and V_F.

$$V_{GX}=\alpha\, C_{EX} + (1-\alpha)\, C_{FX}$$

$$V_{GY}=\alpha\, C_{EY} + (1-\alpha)\, C_{FY},$$

where α now corresponds to the distance between locations E and G divided by the distance between locations E and F.

After the interpolated calibration vectors have been calculated and stored for each pixel, the phantom 56 is replaced with a printed circuit board (PCB) 14 containing a solder joint 22 to be inspected. Solder joints 22 are commonly placed on both sides of printed circuit board 14, such as shown in FIG. 23, with solder joint A being on the top of the board, and solder joint B being on the bottom of the board. In this example, solder joint A is to be inspected and therefore it is positioned in the same plane that the dots 58 on the phantom 56 were located.

Eight transmission images are acquired of the solder joint A in a manner identical to the image acquisition for the phantom 56. This set of images is referred to as the real PCB images. As shown by the four example images (I_1, I_3, I_5, I_7) in FIG. 23, the x-ray projection of the two solder joints A and B shows significant parallax, resulting in a relative displacement of the two solder joints in the images.

The eight real PCB images are then corrected by applying the stored interpolated calibration vectors to each pixel of the real PCB images. The location of the jth pixel of a

corrected PCB image is designed as r_j. The interpolated calibration vector V (r_j) is then subtracted from the corresponding pixel location r_j resulting in a real PCB pixel location T_j. The corrected PB image comprises transferring the grey level for each pixel located at T_j in the real PCB image to pixel location r_j in the corrected PCB image. Because of this procedure, the corrected PCB images are both spatially undistorted and spatially calibrated representations of the image plane. The calculations for the calibration or "dewarping" procedure described with respect to FIGS. 15-22 is performed by a microprocessor 62 shown in FIG. 16.

As shown by the four corrected images in FIG. 24, the image correction translates solder joint A (the solder joint in the image plane) to the same relative location in each of the corrected images. Solder joint B and other objects that are not in the image plane will appear in the corrected image; however, they will not be in the same location in each of the images.

Once the corrected PCB images are stored and the angles θ and ϕ are determined for each of the imaging positions for the x-ray source, one can produce an improved three-dimensional density reconstruction of an object of interest when images are taken from two or more of the imaging positions. For example, as disclosed in U.S. Patent No. 5,500,886, with the values of θ and ϕ known one can accurately determine a particular coordinate, such as Z, for a particular object of interest, such as a solder joint 22, from two or more images of the solder joint taken at the predetermined beam directions. Determining the value of Z is important for x-ray imaging techniques which analyze density distributions at particular positions along the direction between the source and imaging device, since the value of Z is often required. In the past, the value of Z for a solder joint 22 on a circuit board 14 would be determined from a topographical map formed via a laser range finder before an x-ray image was formed. Thus, one can simultaneously determine Z while x-ray images of the solder joint 22 are taken. This results in improved processing times.

The determination of Z is best shown in FIGS. 27-29, in which the image of a solder joint on a circuit board is taken from two or more predetermined x-ray imaging directions. A first source of radiation, such as x-ray source 2, generates a first beam of radiation, such as x-ray beam 24, directed at angles θ_1, ϕ_1 towards the solder joint 22. Next, a second source of radiation, such as x-ray source 2, generates a second beam of radiation, such as x-ray beam 24, directed at angles θ_2, ϕ_2 towards the solder joint 22 as well. The x-rays modulated by the solder joint 22 are directed to an image detector, such as image intensifier 28, for producing 1) a first image (I_1) of the solder joint formed by the first beam of x-rays and 2) a second image

(I_2) of the solder joint formed by the second beam of x-rays. As shown in FIGS. 28 and 29, when the two images of the solder joint 22 are overlapped, they are separated from each other by a length L. A microprocessor 66 (FIG. 16) can determine the pixel positions of the two images of the solder joint 22 and then determines the separation distance L in a well-known manner and determines Z from the values of θ_1, θ_2, ϕ_1, ϕ_2 and L, as follows:

$$Z = L/(\tan^2\theta'_1 + \tan^2\theta'_2 - 2\tan\theta'_1\tan\theta'_2\cos(\phi'_2-\phi'_1))^{1/2}$$

The primes have been added to the angle variables to account for parallax effects. θ and ϕ are known for the center of each image gathered by the view selector. For an image I_1 (i=1,2) off center and located at x,y coordinates X_i and Y_i measured with respect to a point where beam axis 25 intersects the ith image.

$$\tan\theta'_i = [(X_i + Z_1\tan\theta_i\cos\phi_1)^2 + (Y_i = Z_1\tan\theta_i\sin\phi_i)^2]^{1/2}/Z_1 \text{ and}$$

$$\phi'_i = \tan^{-1}[(X_i + Z_1\tan\theta_i\cos\phi_i)/(Y_i + Z_1\tan\theta_i\sin\phi_i)]$$

Z_1 is the distance from x-ray source 2 to object plane 48 and the inverse tangent operation selects the proper value from a full 360° range. It should be noted that Z_1 corresponds to the distance between the x-ray source 2 and object plane 48 as shown in FIG. 5. The above described system for determining Z is described in U.S. Patent No. 5,500,886.

The corrected PCB images, with or without the value of Z known, are mathematically combined to form a reconstructed image. In the ideal case, the reconstructed image only contains information about objects located in a plane of interest. The reconstruction process extracts information in each of the corrected PCB images about this plane and discards all other image information. It is known from the principles of Computed Tomography that this separation of information cannot be perfect and that there will always be artifacts within the reconstructed image. In the prior art systems modeled after diagnostic medical x-ray devices, uncorrected PCB images are simply added together, resulting in reconstructed images with serious artifacts.

The presently preferred embodiments produce reconstructed images with significantly fewer objectionable artifacts. This results from the previously described procedures for creating corrected PCB images in conjunction with a reconstruction procedure specifically suited for PCB inspection. During the image reconstruction step, two or more corrected transmission images, preferably eight, (four of which are shown in FIGS. 24-26) are combined to form a single reconstructed transmission image. As shown in FIG. 25, the simplest way to combine the images is to calculate each pixel in the reconstructed transmission image as the sum of the eight corresponding pixels in the eight corrected

transmission images. Since solder joint A appears at the same location in each corrected transmission image, a simple summation will result in solder joint A appearing very dark in the reconstructed transmission image. Conversely, since solder joint B appears at various locations in the eight corrected images, it will appear to be duplicated eight times in the summation image. Since the eight B solder joint images do not lie upon each other, they will have a high gray scale value for each corresponding pixel, nearly as high as the regions in the image that do not represent a solder joint. Since solder joint A is what is being examined, the duplicated and diluted images of solder joint B are classified as artifacts. These artifacts degrade the ability of the system to produce an image of the solder joint being inspected.

Rather than simply summing eight corresponding pixels to form a single pixel in the reconstructed transmission image, a microprocessor 66 (FIG. 16) combines the pixels in a non-linear manner. As shown in FIG. 26, the pixel having a value corresponding to the least attenuation (largest gray level in value) of the group of eight corresponding pixels is calculated and that single pixel (gray scale) value is transferred to the reconstructed imager. This means that each pixel in the reconstructed transmission image comes from one of the eight corrected images. Since solder joint A appears at the same location in each of the eight corrected images, it appears much the same in the reconstructed transmission image as it does in each of the corrected images. Since solder joint B appears at various locations in the corrected images, the maximum value operator effectively selects image pixels that remove this solder joint's appearance from the reconstructed transmission image. This results in the reconstructed transmission image being much more free from detrimental artifacts.

The three-dimensional construction of a PCB mounted solder connection is nearly binary in x-ray attenuation characteristics. Each volume element (voxel) can be modeled as being entirely filled with either metal (i.e. solder or metal wire), or a low x-ray attenuation material (i.e. air, plastic, organic material, etc.). This is drastically different from the three-dimensional construction of the human body. In this case, all voxels contain material that have similar x-ray attenuation characteristics. Medical x-ray techniques are designed to extract information bout small changes in x-ray attenuation in regions that are submerged in large regions of similar characteristics.

Each pixel in the reconstructed image is calculated from a set of projection pixels. The set of projection pixels consists of the pixels in the corrected PCB images that have the same row and column image address as does the pixel in the reconstructed image. For example, if there are 8 corrected PCT images, a set of projection pixels consists of 8 pixels, one from each of the corrected PCB images. Each of these 8 pixels contains identical

information about the image plane. In each addition, each of the 8 pixels contains information unrelated to the image plane and is not the same in the 8 pixels. In prior art systems, these 8 pixels would simply be added together. This reinforces the information in the image plane since it is identical in all pixels. It also dilutes the non-image plane information since that information is more-or-less random.

In the presently preferred embodiments, each pixel in the reconstructed image is taken to be the gray scale value of the pixel in the set of projection pixels that has the maximum gray scale value. Having the maximum value corresponds to the radiant energy having passed through the lest amount of material. Since each of the pixels in the set of projection pixels contains identical information bout the image plane, the pixel with the maximum value will be least contaminated with non-image plane information. In this manner, the maximum value operator selects those pixels that contain the greatest information about the image plane while rejecting those pixels that have the largest amount of artifacts.

Methods similar to this maximum value reconstruction have been used in medical applications for imaging the human body (for example, "Reconstruction of blood vessels from x-ray subtraction projections: Limited angle geometry", Kruger, Reinecke, Smith, and Ning, Medical Physics, 14(6), Nov/Dec 1987). A preferred embodiment is distinguished from these medical uses because of the unique nature of PCB inspection. The combination of the maximum value reconstruction technique with the unique imaging characteristics of solder connections produces unexpected results that could not have been anticipated form prior art medical uses alone.

While the invention has been described with relation to certain presently preferred embodiments, it is understood that the invention as expressed in the claims is not limited to those described preferred embodiments. Those with skill in this art will recognize other modifications of the invention which will still fall within the scope of the invention, as expressed in the accompanying claims. For example, it is understood that other source and detector configurations are possible, such as a source and detector that are sequentially repositioned to several predefined locations around the image plane such that the dots can be viewed at several distinct angles. At each of these locations, the source and detector are held stationary while a radiant energy image of an object is acquired and digitally stored in the computer.

We claim:

1. A method of imaging a region of interest that is positioned on or within a test object, comprising the steps of:

generating a radiation beam; and

directing the radiation beam to a discrete number of predetermined locations on the test object, wherein the predetermined locations are selected to produce an unobscured electronic image of the region of interest, and wherein the discrete number of predetermined locations is minimized while being of sufficient number to produce the unobscured electronic image.

2. A method as claimed in claim 1, further comprising the step of forming an electronic representation of the region of interest, for each of the predetermined locations of the radiation beam, by detecting a portion of the radiation beam that is transmitted through the region of interest.

3. A method as claimed in claim 2, further comprising the step of forming a composite image, the composite image comprising a combination of the electronic representations of the region of interest.

4. A method as claimed in claim 1, wherein the radiation beam comprises an x-ray beam.

5. A method as claimed in claim 4, wherein said directing step comprises directing an electron beam to a discrete number of predetermined locations on a target in an x-ray tube.

6. A method as claimed in claim 5, wherein said discrete number of predetermined locations on the target form a noncircular pattern.

7. A method as claimed in claim 6, wherein the noncircular pattern is linear.

8. A method as claimed in claim 4, wherein said directing step comprises physically moving at least one of an x-ray tube, the test object and a detector to a discrete number of predetermined locations.

9. A method as claimed in claim 8, wherein the x-ray tube is moved, in relation to the test object, to the discrete number of predetermined locations.

10. A method as claimed in claim 8, wherein the test object is moved, in relation to the x-ray tube, to the discrete number of predetermined locations.

11. A method as claimed in claim 8, wherein moving the detector comprises the step of rotating a pair of mirrors to bring a different portion of an image intensifier into a field of view.

12. A method as claimed in claim 8, wherein moving the detector comprises the step of displacing the detector in relation to the test object.

13. A method as claimed in claim 1, wherein said test object is a circuit board.

14. A method as claimed in claim 13, wherein said region of interest comprises a solder connection on said circuit board.

15. A method as claimed in claim 13, wherein said region of interest comprises a component on said circuit board.

16. A method as claimed in claim 1, wherein the predetermined locations are determined in accordance with a geometry of an obscuring body located outside of the region of interest.

17. An apparatus for imaging a region of interest that is positioned on or within a test object, comprising:

means for generating a radiation beam; and

means for directing the radiation beam to a discrete number of predetermined locations on the test object, wherein the predetermined locations are selected to produce an unobscured electronic image of the region of interest, and wherein the discrete number of predetermined locations is minimized while being of sufficient number to produce the unobscured electronic image.

18. An apparatus as claimed in claim 17, wherein said generating means comprises an x-ray tube.

19. An apparatus as claimed in claim 18, wherein said directing means comprises a controller that steers an electron beam within the x-ray tube to a corresponding discrete number of predetermined locations on a target within the x-ray tube.

20. An apparatus as claimed in claim 17, further comprising a loading device, the loading device being operable to position a series of test objects within the radiation beam.

21. An apparatus as claimed in claim 20, wherein said loading device comprises a shuttle assembly.

22. An apparatus as claimed in claim 21, wherein said shuttle assembly comprises a conveyor and a radiation guard.

23. An apparatus as claimed in claim 22, wherein the radiation guard comprises two opposing walls that are pivotable about a common point.

24. An apparatus as claimed in claim 12, wherein the radiation guard comprises a lead sheet and the radiation guard is positioned to block radiation from the generating means.

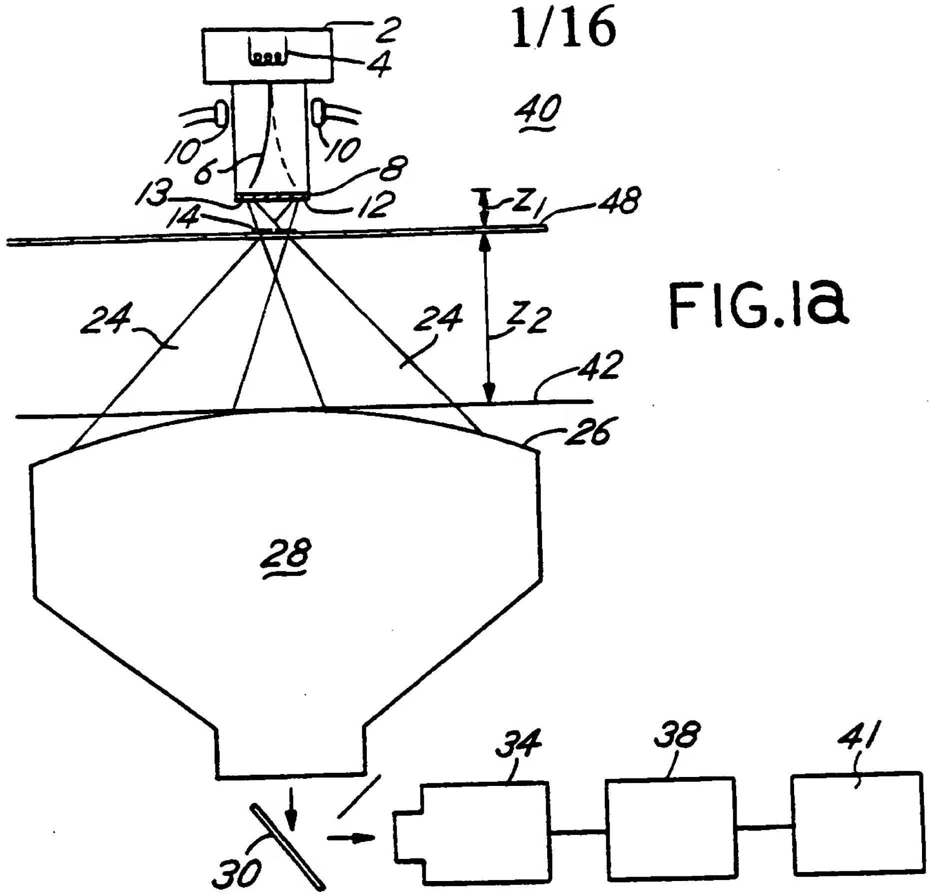
2
4
40
10
10
6
8
13
12
14
Z1
48
24
24
Z2
42
26
28
34
38
41
30

FIG.1a

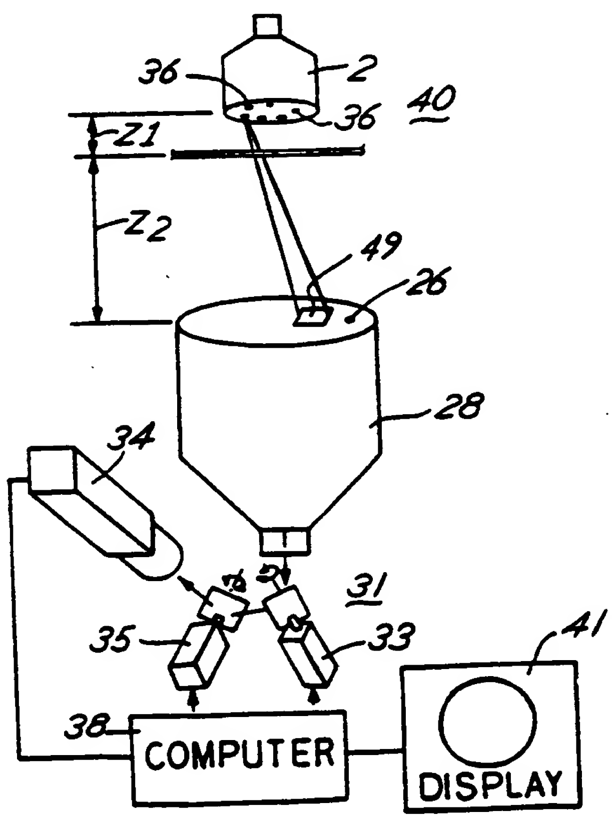
36
2
36
40
Z1
Z2
49
26
28
34
31
35
33
41
38
COMPUTER
DISPLAY

FIG.1b

FIG. 2

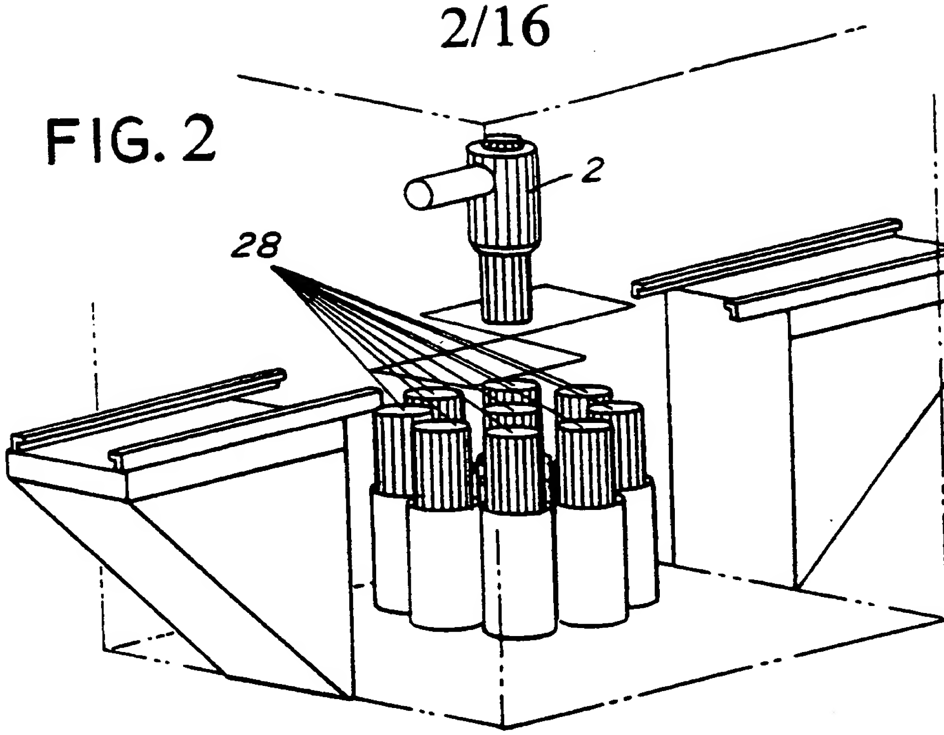
2
28

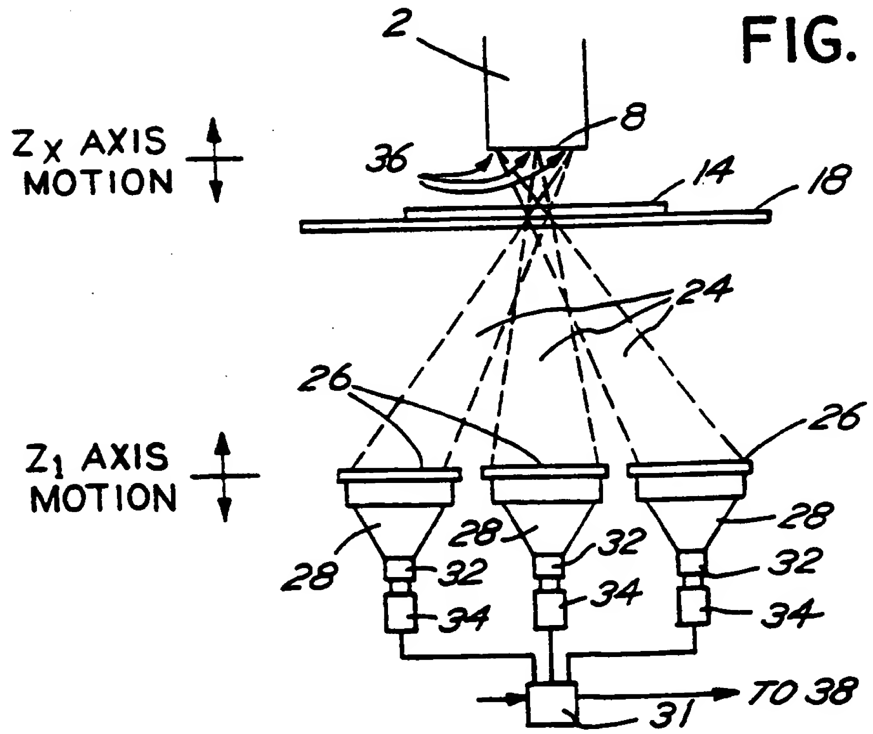
2
8
Z_X AXIS MOTION
36
14
18
24
26
26
Z_1 AXIS MOTION
28
28
28
32
32
32
34
34
34
31
TO 38

FIG. 1C

FIG. 3

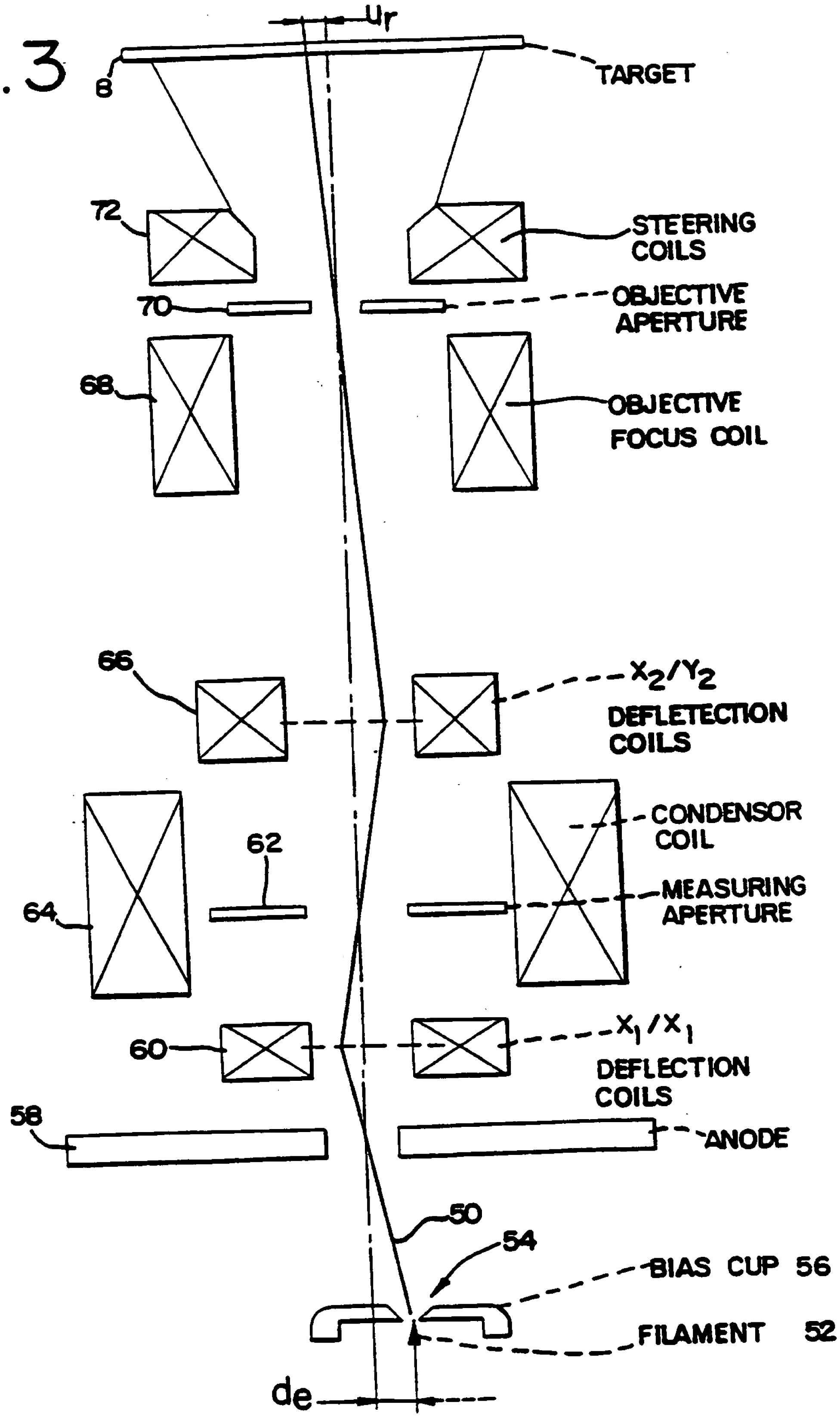

ur
8
TARGET
72
STEERING COILS
70
OBJECTIVE APERTURE
68
OBJECTIVE FOCUS COIL
66
X2/Y2 DEFLETECTION COILS
CONDENSOR COIL
62
64
MEASURING APERTURE
60
X1/X1 DEFLECTION COILS
58
ANODE
50
54
BIAS CUP 56
FILAMENT 52
de

FIG. 4A

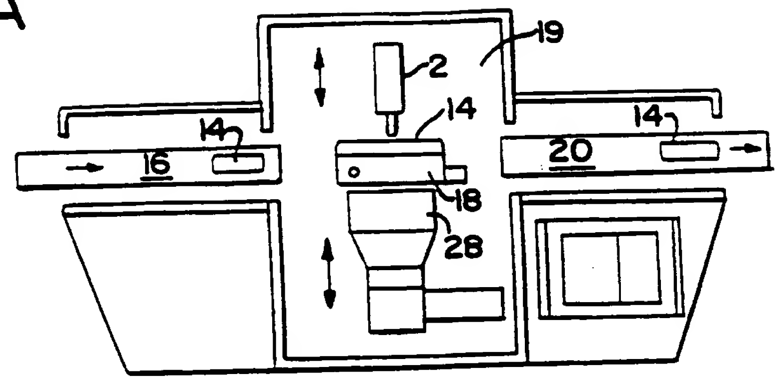

FIG. 4B

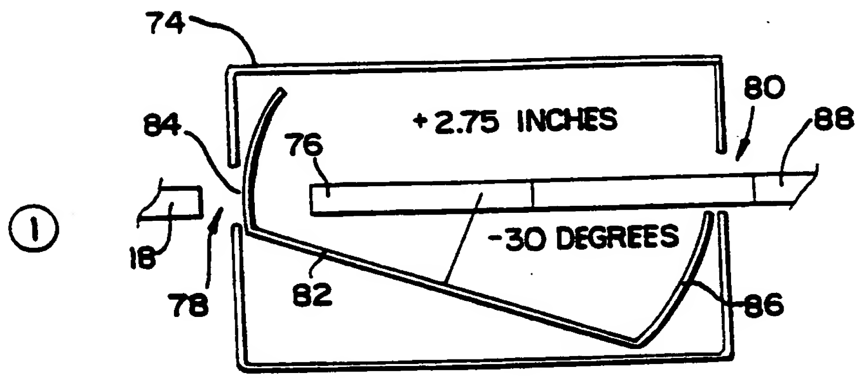

FIG. 4C

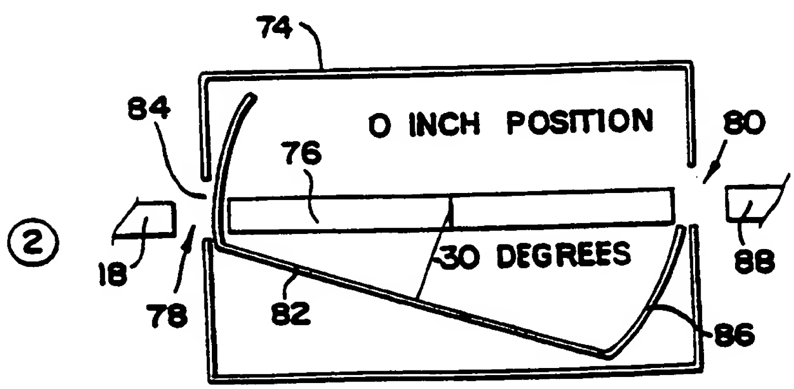

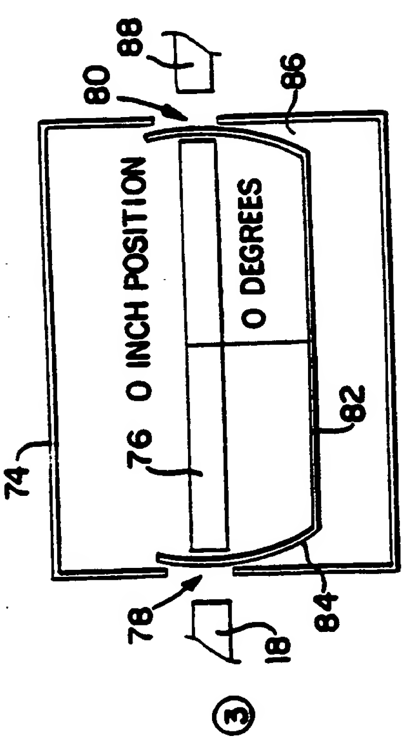

FIG.4D

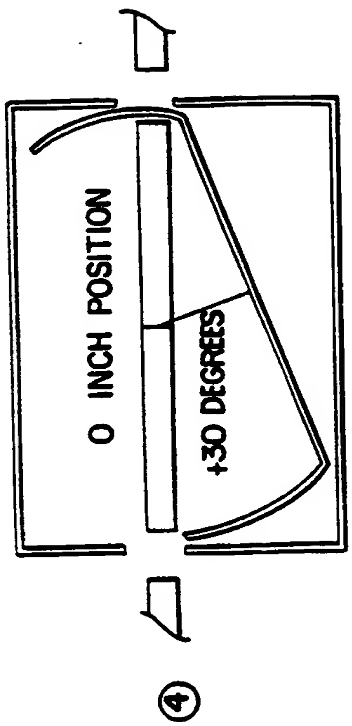

FIG. 4E

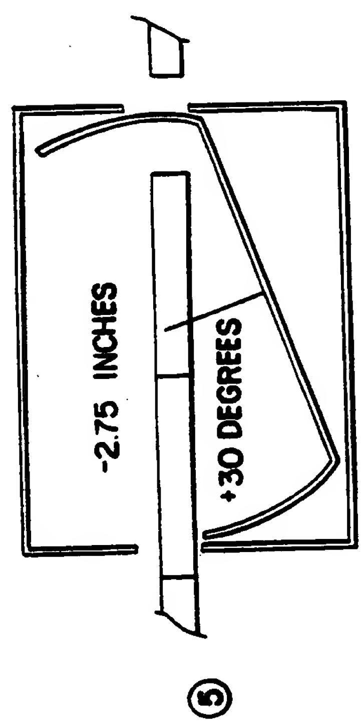

FIG.4F

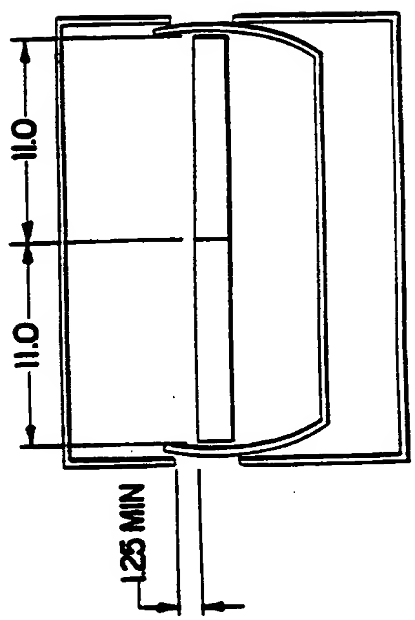

FIG. 4G

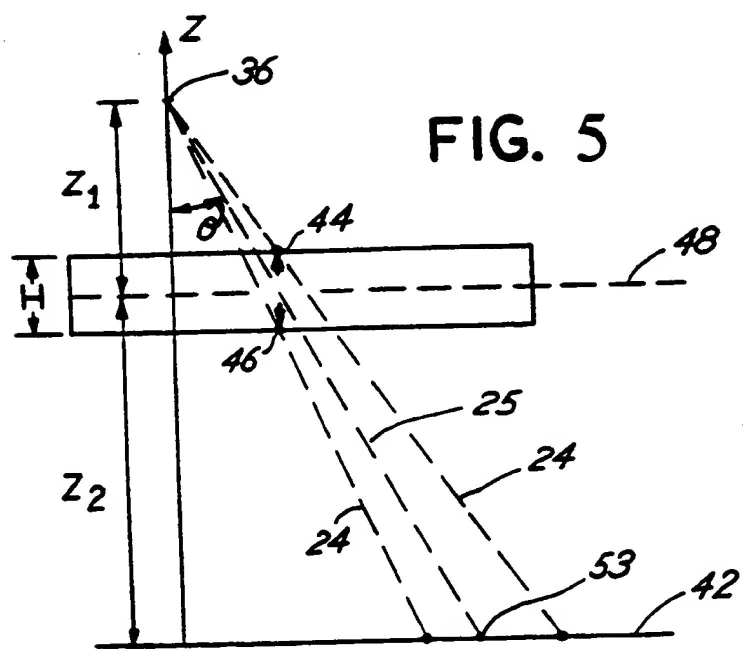

FIG. 5

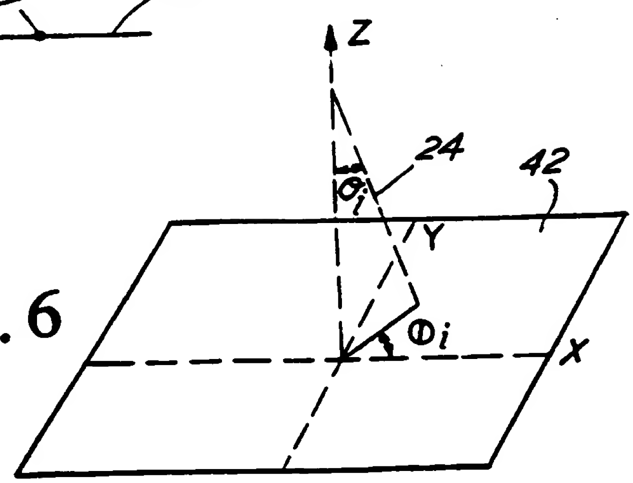

FIG. 6

FIG.7

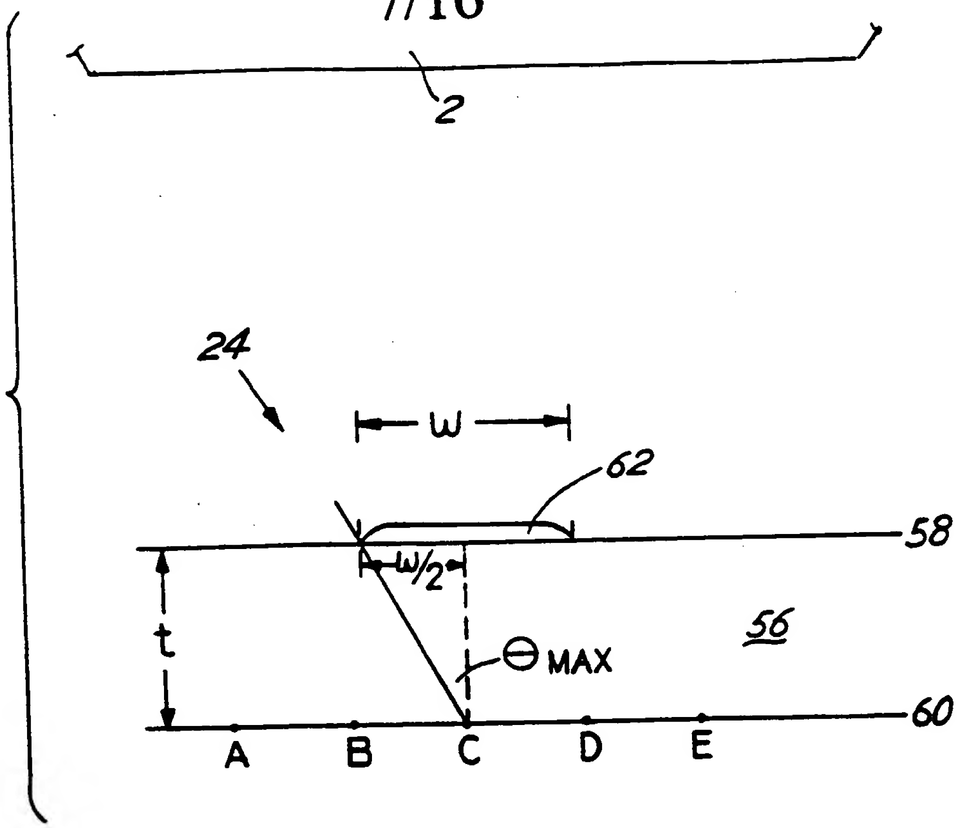

2
24
W
62
58
W/2
t
56
Θ MAX
60
A
B
C
D
E

FIG.8

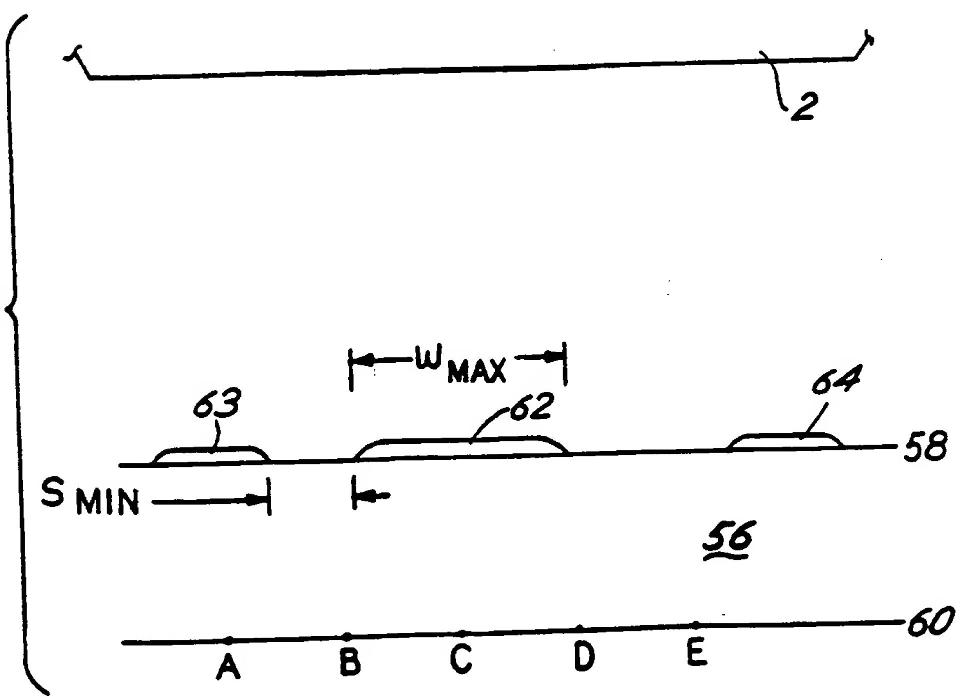

2
W MAX
64
63
62
58
S MIN
56
60
A
B
C
D
E

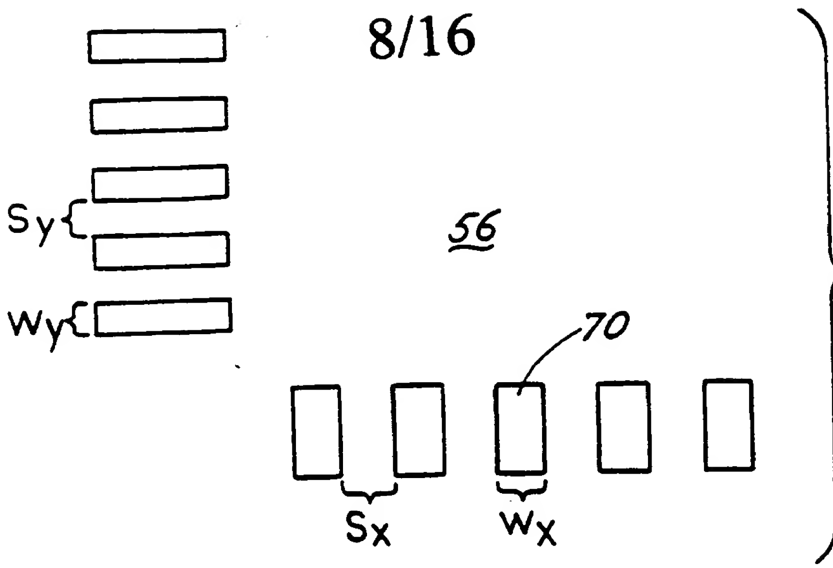

FIG. 9

FIG. 10

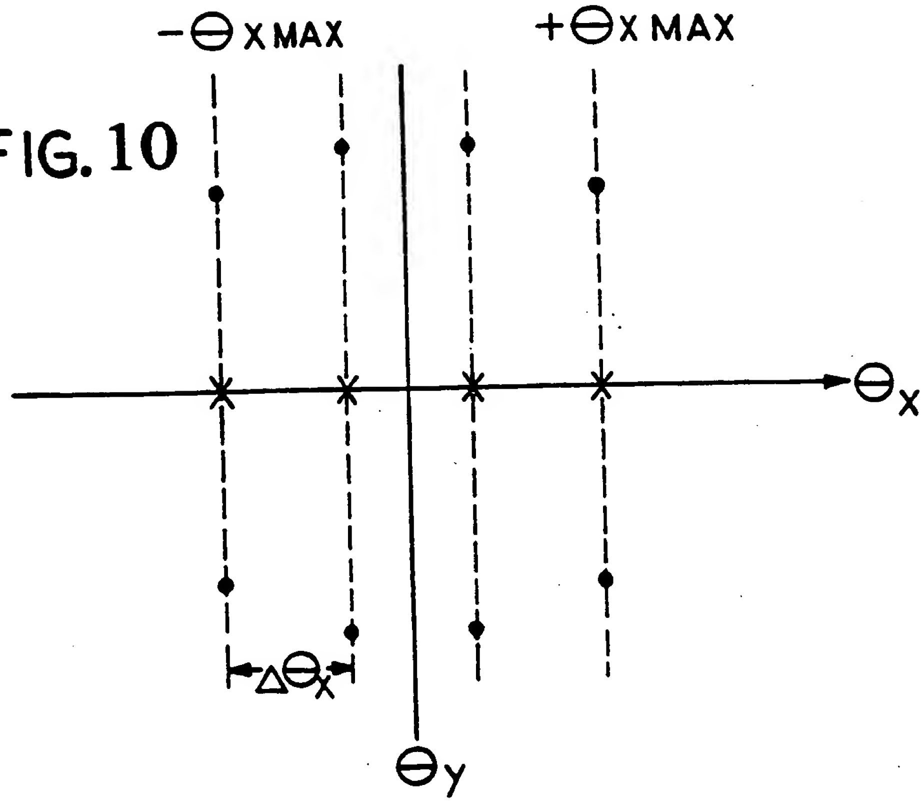

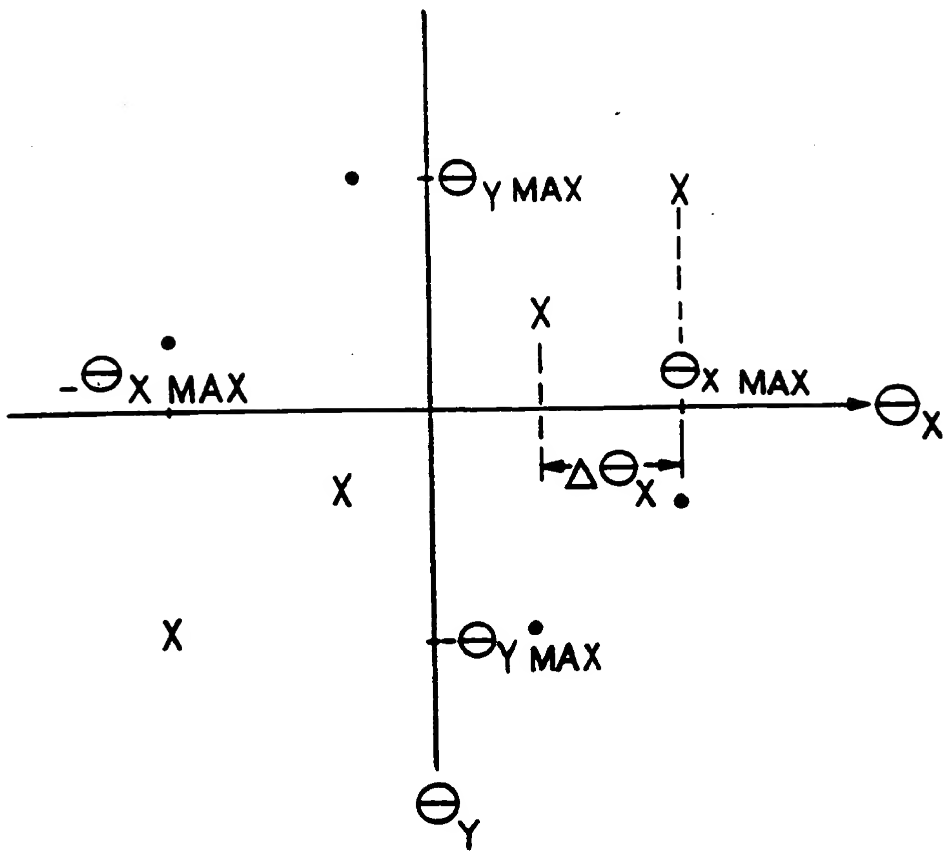

Θ_Y MAX
X
X
$-\Theta_X$ MAX
Θ_X MAX
Θ_X
$\Delta\Theta_X$
X
X
$-\Theta_Y$ MAX
Θ_Y

FIG. 11

FIG. 12

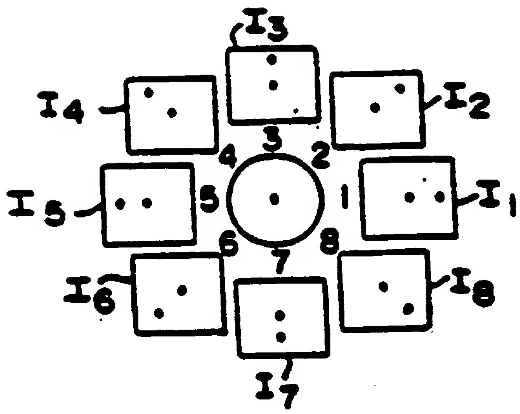

FIG. 13

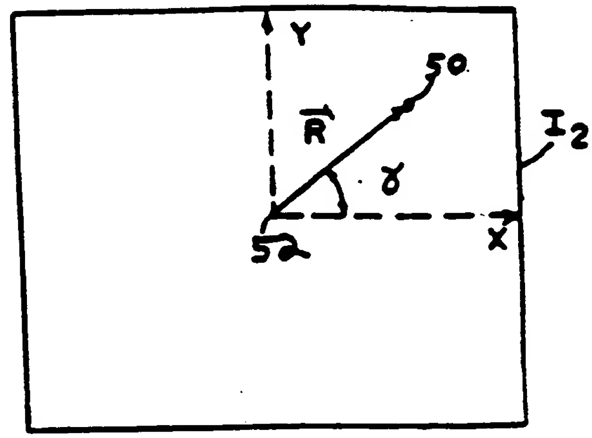

FIG. 14

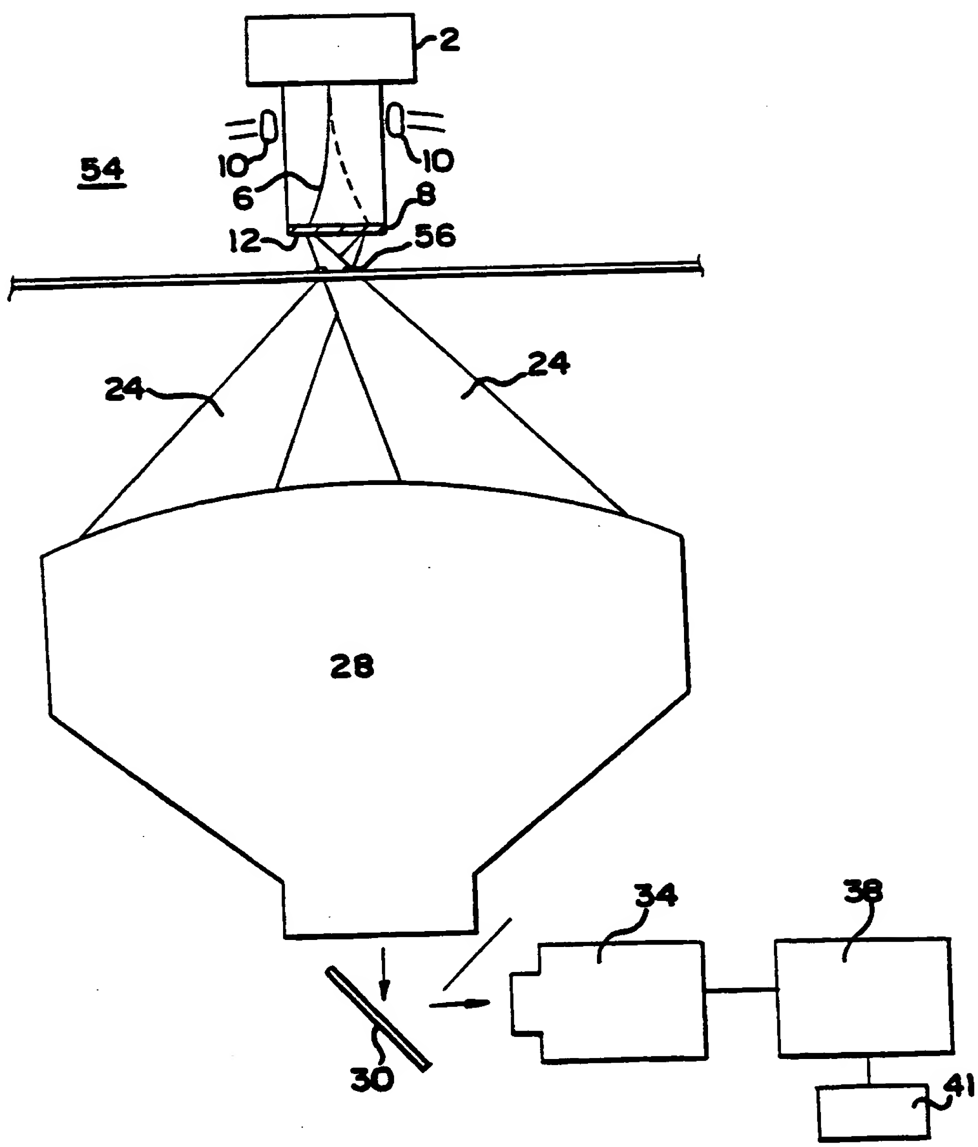

FIG. 15

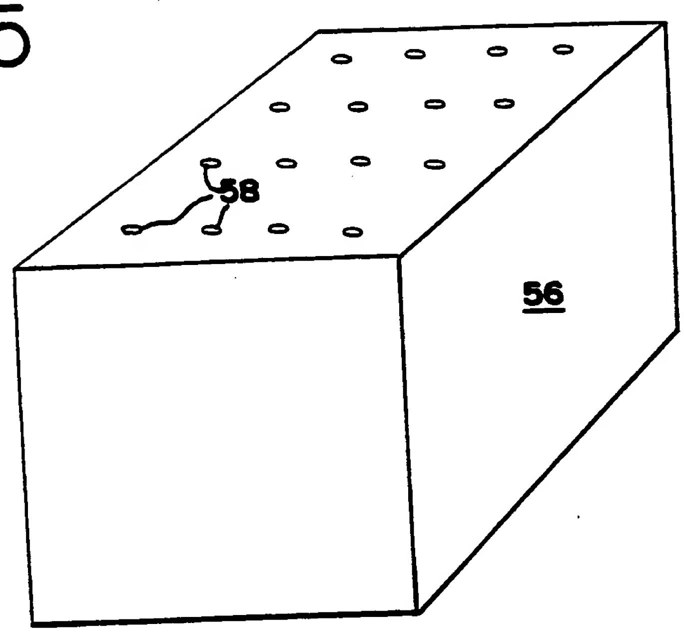
58
56

FIG. 16

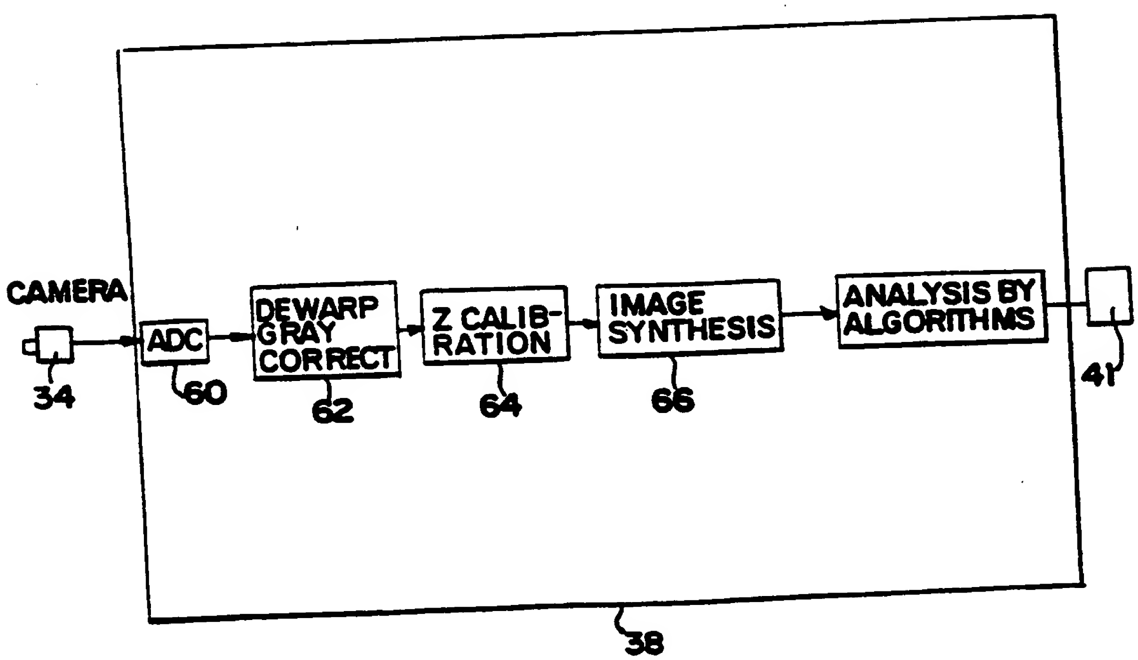
CAMERA
ADC
DEWARP GRAY CORRECT
Z CALIB-RATION
IMAGE SYNTHESIS
ANALYSIS BY ALGORITHMS
34
60
62
64
66
41
38

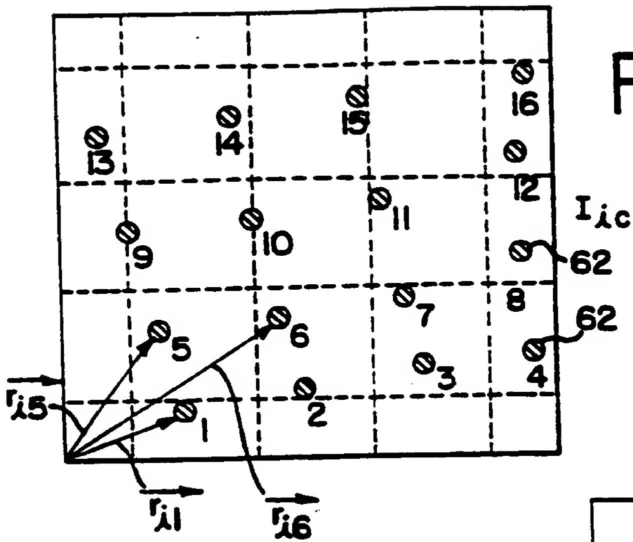

FIG.17

FIG.18

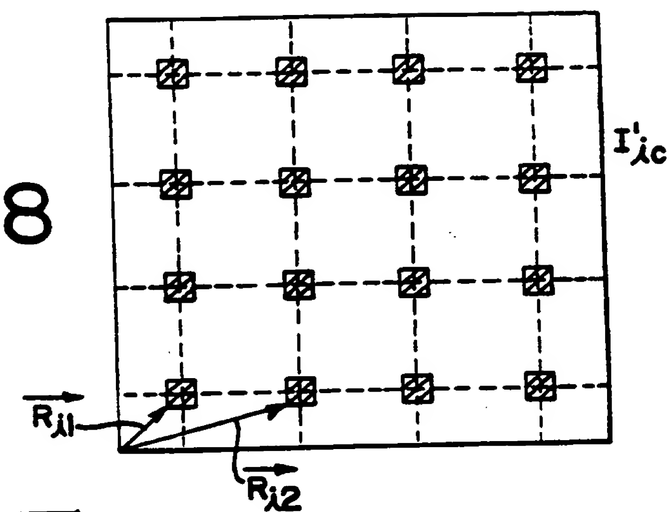

FIG.19

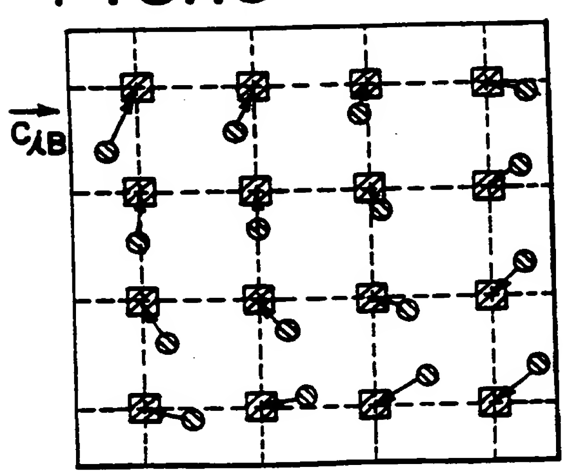

FIG.20

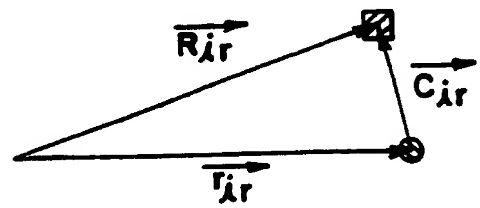

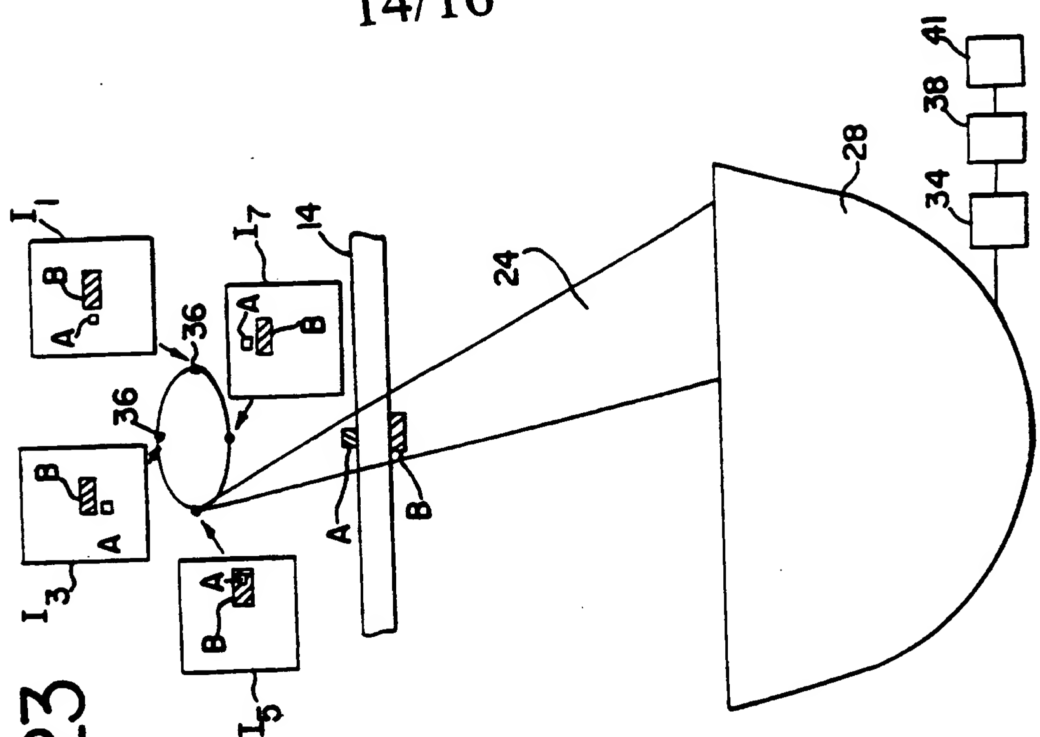

FIG.23

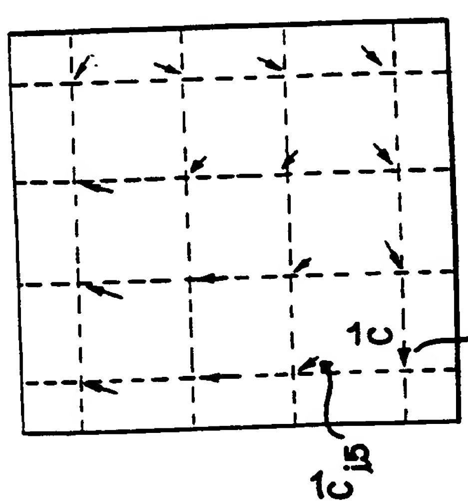

FIG.21

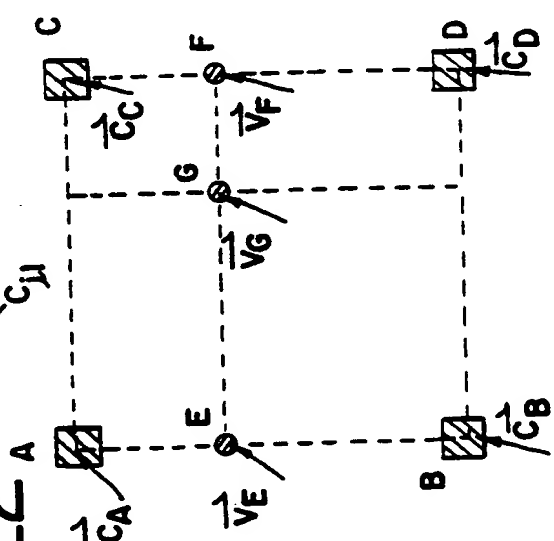

FIG.22

FIG.26

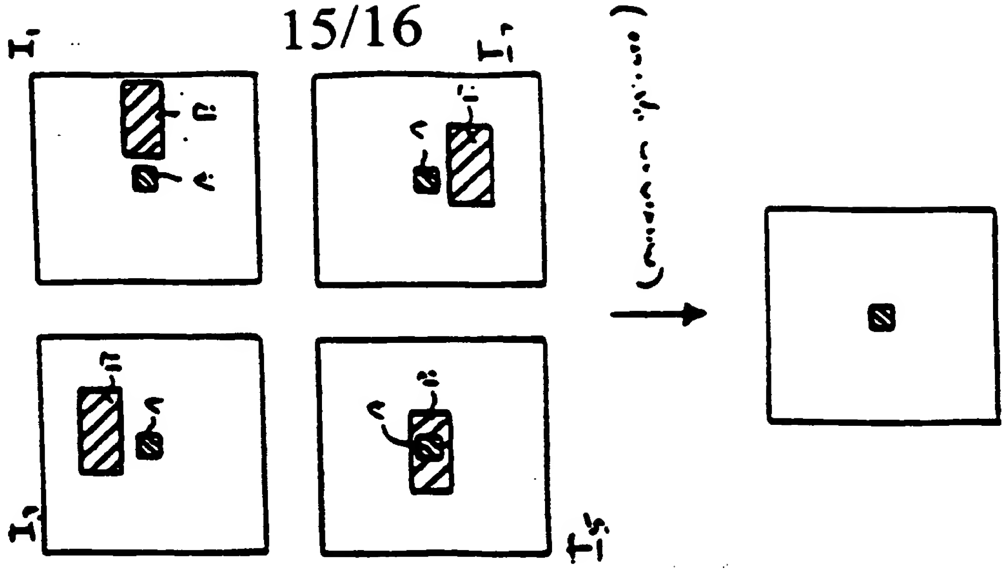

FIG.25

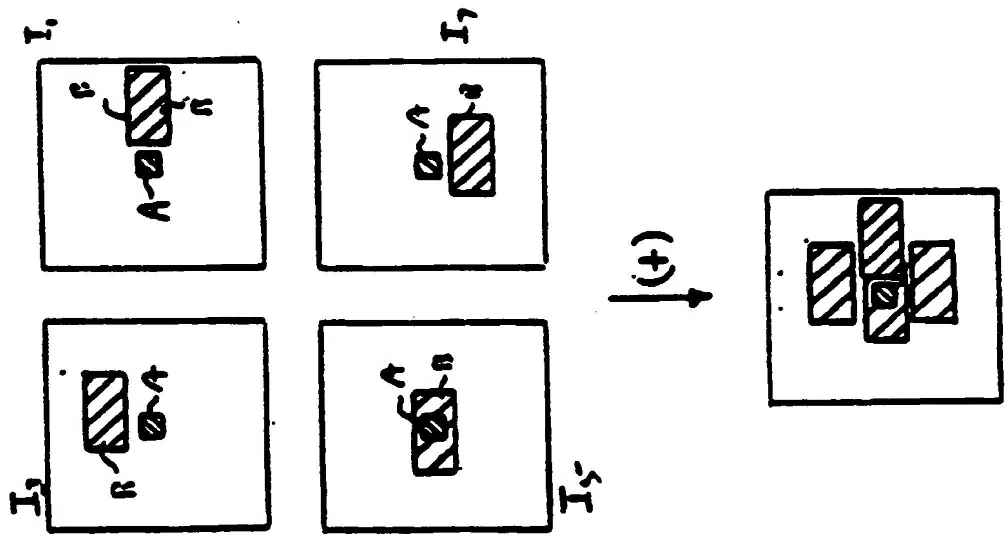

FIG.24

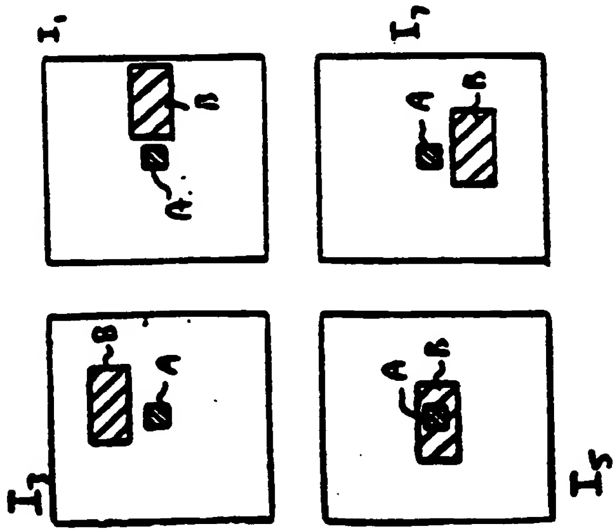

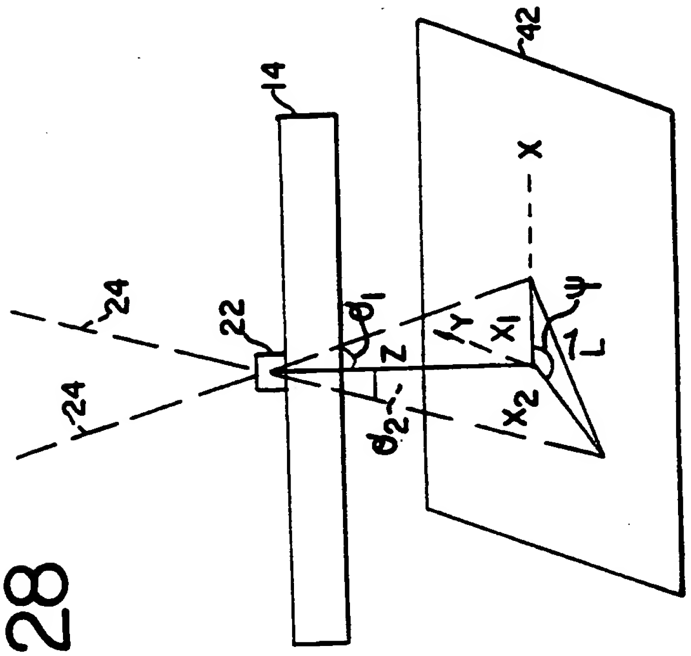

FIG.28

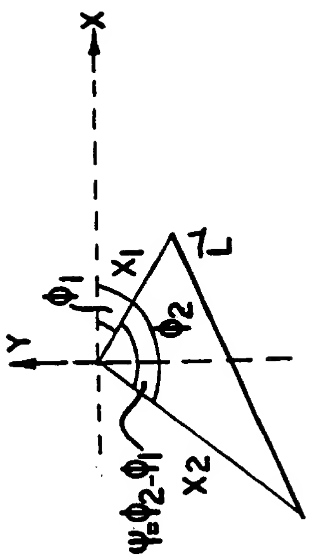

FIG.29

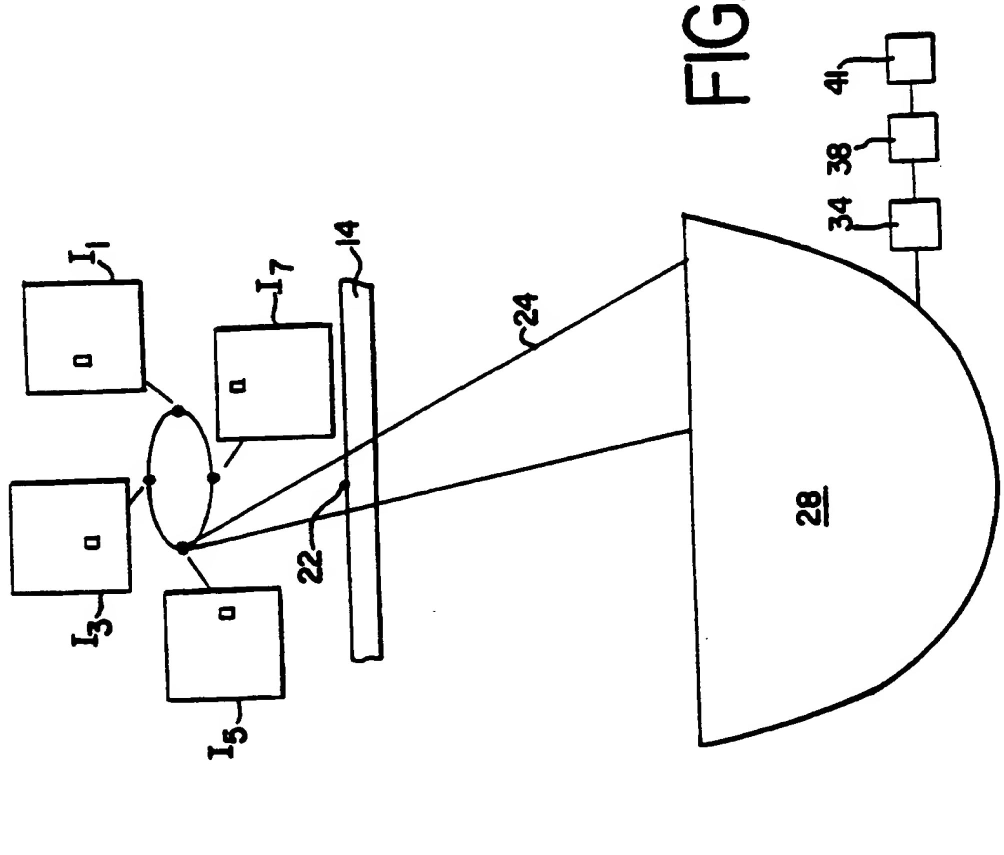

FIG.27

INTERNATIONAL SEARCH REPORT

International Application No
PCT/US 99/03269

A. CLASSIFICATION OF SUBJECT MATTER
IPC 6 G01N23/04

According to International Patent Classification (IPC) or to both national classification and IPC

B. FIELDS SEARCHED

Minimum documentation searched (classification system followed by classification symbols)
IPC 6 G01N

Documentation searched other than minimum documentation to the extent that such documents are included in the fields searched

Electronic data base consulted during the international search (name of data base and, where practical, search terms used)

C. DOCUMENTS CONSIDERED TO BE RELEVANT

Category °	Citation of document, with indication, where appropriate, of the relevant passages	Relevant to claim No.
X	US 5 594 770 A (BOWLES PHILIP ET AL) 14 January 1997 (1997-01-14) column 1, line 56 - column 2, line 10 column 3, line 31 - line 53 column 5, line 3 - line 14 column 7, line 41 - line 49 column 8, line 7 - line 9 column 10, line 46 - column 11, line 3 claims 1,4-6,28; figures	1-9,11, 13,14, 16-20
Y		21,24

Y	US 5 491 737 A (YARNALL RANSOM A ET AL) 13 February 1996 (1996-02-13) cited in the application column 3, line 34 - line 61 figure 1	21,24

☐ Further documents are listed in the continuation of box C.

☒ Patent family members are listed in annex.

° Special categories of cited documents :

"A" document defining the general state of the art which is not considered to be of particular relevance

"E" earlier document but published on or after the international filing date

"L" document which may throw doubts on priority claim(s) or which is cited to establish the publication date of another citation or other special reason (as specified)

"O" document referring to an oral disclosure, use, exhibition or other means

"P" document published prior to the international filing date but later than the priority date claimed

"T" later document published after the international filing date or priority date and not in conflict with the application but cited to understand the principle or theory underlying the invention

"X" document of particular relevance; the claimed invention cannot be considered novel or cannot be considered to involve an inventive step when the document is taken alone

"Y" document of particular relevance; the claimed invention cannot be considered to involve an inventive step when the document is combined with one or more other such documents, such combination being obvious to a person skilled in the art.

"&" document member of the same patent family

Date of the actual completion of the international search	Date of mailing of the international search report
28 July 1999	04/08/1999

Name and mailing address of the ISA	Authorized officer
European Patent Office, P.B. 5818 Patentlaan 2 NL - 2280 HV Rijswijk Tel. (+31-70) 340-2040, Tx. 31 651 epo nl, Fax: (+31-70) 340-3016	Krametz, E

1

INTERNATIONAL SEARCH REPORT

Information on patent family members

onal Application No

PCT/US 99/03269

Patent document cited in search report		Publication date	Patent family member(s)	Publication date
US 5594770	A	14-01-1997	NONE	
US 5491737	A	13-02-1996	NONE	

THIS PAGE BLANK (USPTO)